Immunomodulation of Tumor Associated Macrophages by Targeted, siRNA-Delivering Nanoparticles

By

Ryan Adam Ortega

Dissertation

Submitted to the Faculty of the

Graduate School of Vanderbilt University

in partial fulfillment of the requirements

for the degree of

DOCTOR OF PHILOSOPHY

In

Biomedical Engineering

December, 2014

Nashville, Tennessee

Approved:

Todd D. Giorgio, Ph.D.

Fiona E. Yull, D.Phil.

Craig L. Duvall, Ph.D.

Barbara Fingleton, Ph.D.

Frederick R. Haselton, Ph.D.

TABLE OF CONTENTS

LIST OF TABLES

Table Page

LIST OF FIGURES

LIST OF ABBREVIATIONS

TAM	Tumor associated macrophage
BMDM	Bone marrow derived macrophage
M1	Classically activated macrophage; pro-inflammatory
M2	Alternatively activated macrophage
NK cell	Natural killer cell
PMN cell	Polymorphonuclear cell; granulocyte
siRNA	Small interfering RNA
RNAi	RNA interference
NF-κB	Nuclear factor kappa-light-chain-enhancer of activated B cells
p105/p50 (NF-κB1)	Class 1 NF-κB protein of the classical NF-κB pathway
p100/p52 (NF-κB2)	Class 1 NF-κB protein of the alternative NF-κB pathway
p65 (RelA)	Class 2 NF-κB protein of the classical NF-κB pathway
RelB	Class 2 NF-κB protein of the alternative NF-κB pathway
IκBα	Inhibitor of the NF-κB transcription factor; inhibitor of classical NF-κB pathway
IKKα (IKK1, CHUK)	IκB kinase alpha; activator of classical and alternative NF-κB pathway
IKKβ (IKK2)	IκB kinase beta; activator of classical NF-κB pathway
NEMO (IKKγ)	NF-κB essential modulator; activator of classical NF-κB pathway
NIK	NF-κB inducing kinase; activator of classical NF-κB pathway
TRAF3	TNF receptor-associated factor 3; Inhibitor of NIK
CSF-1 (M-CSF)	Colony stimulating factor 1 (macrophage colony stimulating factor)
LPS	Lipopolysaccharide
IFN-γ	Interferon gamma; immune activating cytokine
TNF-α	Tumor necrosis factor alpha
RANKL	Receptor activator of nuclear factor kappa-B ligand; TNF family member
CD40L	CD40 ligand; TNF family member
TWEAK	TNF-related weak inducer of apoptosis; TNF family member
IL-1	Interleukin 1; pro-inflammatory cytokine
IL-4	Interleukin 4; cytokine promoting alternative macrophage activation
IL-10	Interleukin 10; anti-inflammatory cytokine
IL-12	Interleukin 12; an activator of immune cells
MMP	Matrix metalloproteinase
ROS	Reactive oxygen species
MIF	Macrophage migration inhibitory factor
CCL2 (MCP1)	Monocyte chemotactic protein 1
CCL3 (MIP-1α)	Macrophage inflammatory protein 1 alpha
CSF-1R	CSF-1 receptor; a macrophage surface marker
CD11b (ITGAM)	Integrin alpha M (compliment receptor 3); a myeloid cell surface marker
CD45	Leukocyte common antigen
CD206	Mannose receptor
F4/80	A murine macrophage surface marker
Gr1	A negative macrophage surface marker; lost during macrophage maturation
CD8	A transmembrane binding protein; a marker for cytotoxic T-cells
GAPDH	Glyceraldehyde 3-phosphate dehydrogenase
RAFT	Reversible addition-fragmentation chain transfer
BME	Butyl methacrylate

PAA	Propylacrylic acid
DMAEMA	2-(Dimethylamino)ethyl methacrylate
AzEMA	2-Azidoethyl methacrylate
MnNP	Mannosylated endosomal escape nanoparticle
OHNP	OH terminated endosomal escape nanoparticle
CFSE	Carboxyfluorescein succinimidyl ester
PyMT	Polyoma middle T oncogene
NGL	Transgenic mouse expressing luciferase and GFP as an NF-κB activation readout
HLL	Transgenic mouse expressing luciferase as an NF-κB activation readout
wt	Wild type
qRT-PCR	Quantitative reverse transcription polymerase chain reaction
AST	Aspartate aminotransferase
ALT	Alanine aminotransferase
BUN	Blood urea nitrogen
CREAT	Creatinine
DMEM	Dulbecco's modification of Eagle's medium
FBS	Fetal bovine serum

CHAPTER 1

Tumor associated macrophages as a potential target for nanoparticle-mediated, anti-tumor immunomodulation

Tumor associated macrophages (TAMs) play an important role in establishing a pro-tumorigenic local microenvironment in many tumor types. These macrophages stimulate angiogenesis, promote tumor growth and metastasis, and suppress the normal immune response.[5, 6] TAMs display a phenotype that is a blend of the two classical macrophage phenotypic categories. Like the classically immunogenic (M1) macrophage, TAMs produce low levels of inflammatory cytokines which creates pro-tumorigenic smoldering inflammation.[7] Like the classical description of a tissue remodeling (M2) macrophage, TAMs break down the surrounding extracellular matrix, secrete growth factors, and inhibit the adaptive immune response.[2]

It has been demonstrated that tumor associated macrophages are a viable therapeutic target in cancer treatment and ablating these cells can have a powerful anti-tumor effect.[4] A more elegant solution would be to target these pro-tumor macrophages with a therapeutic agent that can alter their behavior to a strongly immunogenic phenotype capable of stimulating tumor immunity. In order to facilitate this immunological engineering, a target for phenotypic modulation must be elucidated. The NF-κB pathways control macrophage phenotype and the inflammatory response.[8] Tumor cell induced NF-κB deregulation has also been implicated in creating many of the pro-tumor traits of TAMs.[9] By selectively manipulating NF-κB in TAMs, it should be possible to eradicate the TAM phenotype and recapitulate the normal immune response.

siRNA is a potent therapeutic agent that can selectively knock down the translation of specific mRNA into protein.[10] Clinical trials of siRNA therapeutics utilize targeted nanoparticles as a delivery device to reach specific cell populations.[11] A mannose functionalized nanoparticle with an siRNA

condensing region can target the macrophage mannose receptor (upregulated in TAMs) and deliver NF-κB specific siRNAs in order to change the TAM phenotype.[12, 13]

Tumor associated macrophages (TAMs) as a therapeutic target for cancer treatment

The tumor supportive stroma has been identified as an attractive target for therapeutic intervention in breast cancer. In particular, macrophages have been implicated in supporting tumor associated angiogenesis, promotion of local tumor growth and invasion, tumor cell migration, intravasation, and suppression of an anti-tumor immune response.[1, 5, 6] Macrophages play an important trophic role in tissue development and one suggested mechanism for the TAM phenotype is that these roles are recapitulated in the tumor microenvironment.[14] An increase in TAMs at the site of tumor progression has proven to be predictive of poor prognosis and survival in mouse models of human breast cancer.[15, 16]

Over expression of one of the major factors controlling macrophage maturation, CSF-1 (M-CSF), has been associated with poor prognosis in breast, ovarian, prostate, hepatocellular, and colorectal cancer.[1, 17] One of the more insidious characteristics of TAMs driven in part by CSF-1 is their ability to prepare a metastatic niche for circulating tumor cells (Figure 1.1).[1] Ablation of CSF-1 in the polyoma middle T oncogene (PyMT) mouse model of human breast cancer greatly reduces macrophage density in the tumor, resulting in a decreased rate of tumor progression and an inhibition of metastases.[18] In addition to data from studies of CSF-1 in cancer, CCL-2, a major macrophage chemotaxis factor has been shown to be upregulated in a wide range of cancers, and is associated with poor

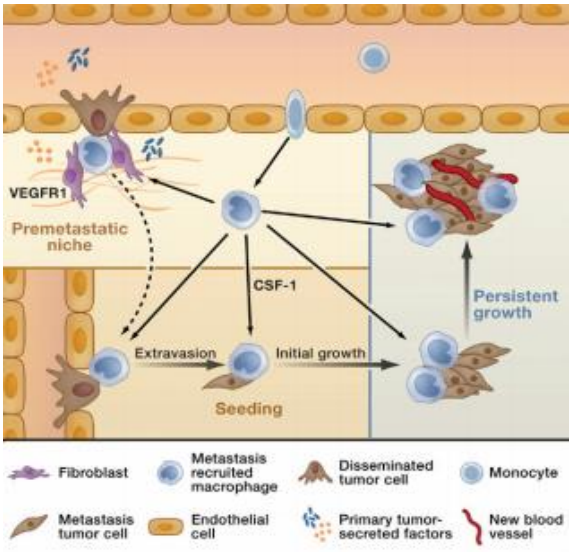

Figure 1.1: Macrophages are recruited to the pre-metastatic niche by secreted products from the primary tumor. Once tumor cells arrive at the metastatic site, they recruit macrophages from the blood. These macrophages accumulate, and promote tumor cell survival and growth. Figure adapted from source #4. [4]

prognosis in breast cancer.[17] Depletion of macrophages reduces tumor growth in melanoma, ovarian cancer, Lewis lung carcinoma, and prostate tumor graft models.[1] All of this evidence supports the role of TAMs as a viable therapeutic target for treating breast cancer. Furthermore, unlike tumor cells, the genomes of macrophages are stable; they may not become resistant to therapy as readily as tumor cells.

Defining the TAM phenotype

TAMs are phenotypically distinct from the classic M1/M2 description of macrophage phenotype, but blend together several characteristics of both. In the classic description of macrophages, M1 or 'classically activated' macrophages are thought of as the pro-inflammatory, immune response-controlling macrophages. M1 activation is associated with an increase in inflammatory cytokines IFN-γ, TNF-α, IL12, chemoattractants for CD8+ T-cells, and reactive oxygen species. This phenotype describes a cell that acts as a first responder to the site of injury or microorganism invasion and controls local inflammation and the total immune response.[2] M2 or 'alternatively activated' macrophages exhibit an increase in scavenger and mannose receptors, an increased production of anti-inflammatory cytokines IL-10 and IL-1 receptor antagonist, and an increased production of T-regulatory cell chemoattractant, CCL-22.[2] The M2 phenotype describes a cell that tunes and inhibits inflammation and the adaptive immune response as well as promotes tissue repair, angiogenesis and tissue remodeling facilitated by increased production of MMP-1 and MMP-9.[19] Many, if not all of these key properties of M2 macrophages are present in TAMs. Alberto Mantovani and collaborators have published a model of TAMs as an M2 macrophage; a summary of their findings are depicted in Figure 1.2.

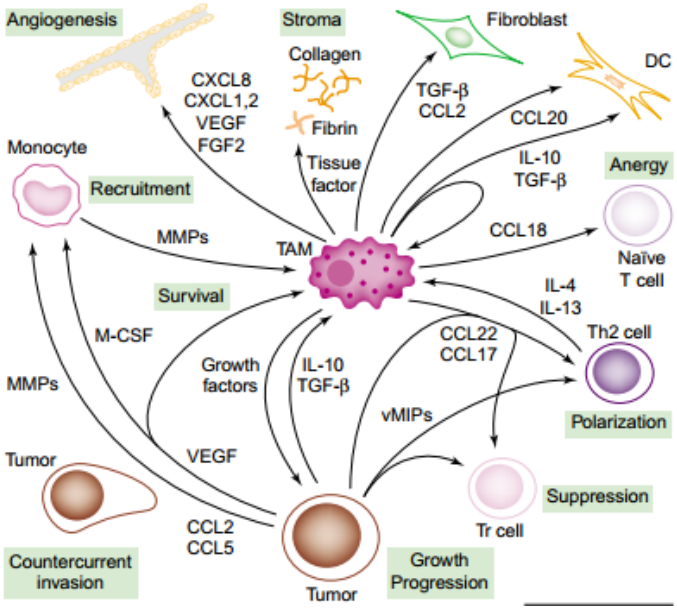

Figure 1.2: TAMs as polarized M2 macrophages. TAMs are a source and target for cytokines and chemokines in the tumor microenvironment. These molecules and other local mediators regulate tumor growth, progression and invasion, interaction with other stromal components, and the activation and orientation of adaptive immunity. Figure adapted from source #2.[2]

Initially, it appears as if the M2 phenotype is a perfect model for the TAM phenotype. However, the M2 phenotype cannot account for one of the defining characteristics of TAMs: smoldering inflammation. Smoldering inflammation is a pro-tumorigenic state characterized by low levels of local inflammation combined with a paradoxical blunting of innate and adaptive immunity.[7, 20] While in a state of smoldering inflammation, a pre-cancerous niche is constantly exposed to reactive oxygen species (ROS), which react with DNA in the surrounding cells resulting in permanent genomic alterations, but not enough to result in cell death. In addition to low levels of ROS and other inflammatory cytokine production, TAMs produce migration inhibitory factor (MIF), a cytokine that overcomes p53 function by suppressing its transcriptional activity.[21] These phenotypic traits are usually associated with M1 macrophages.

The TAM phenotype does not map cleanly onto the classical M1/M2 description of macrophages. Instead it displays a blended phenotype in which traits from both M1 and M2 macrophages are selected to create a strongly pro-tumor microenvironment. TAMs produce growth factors to promote tumor cell growth, tissue remodeling, and angiogenesis. They suppress the immune response to tumor cells while simultaneously creating low levels of local inflammation. When taken together, these traits show that TAMs play a critical role in tumor progression, summarized in Figure 1.3.

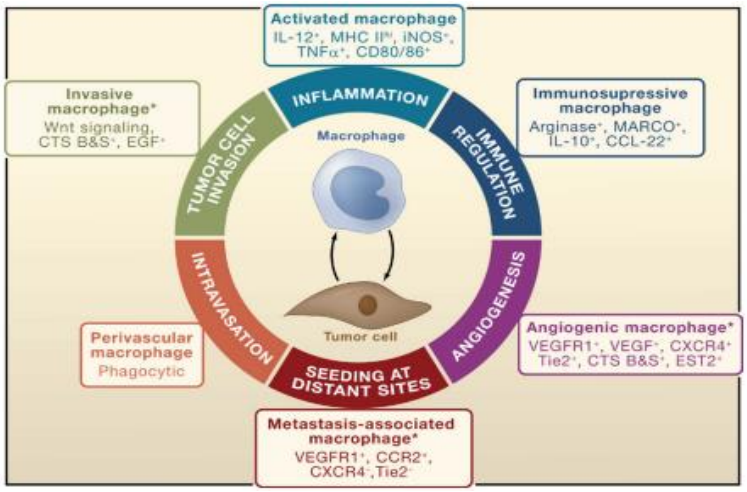

Figure 1.3: Six macrophage functions that provide support to a tumor. All of these macrophage subtypes are defined by the expression of canonical markers CD11b, F4/80, and CSF-1R, and the absence of Gr1, but they are educated by the tumor cells to adopt a TAM phenotype and perform the tasks shown. Figure adapted from source #1.[1]

NF-κB deregulation in macrophages creates a pro-tumor environment

NF-κB is a transcriptional pathway that has been studied for over 25 years and is known to regulate hundreds of genes. This pathway is active in many cell types and plays a major role in controlling the inflammatory response in macrophages in particular.[8] Investigations of NF-κB activation in solid tumors have revealed a critical role for NF-κB in linking inflammation with tumor development.[20] In myeloid cells such as macrophages, the inflammatory state is controlled by NF-κB activation which is essential for the inflammatory macrophage phenotype.[22] NF-κB activation is needed to create many of the traits of TAMs including the critical smoldering inflammation state.[17] The total effect that NF-κB activation in macrophages has on the tumor microenvironment is complicated. The NF-κB pathway is actually comprised of the two parallel pathways seen in Figure 1.4.[3] The classical pathway is well understood and has been studied in great detail; however, the alternative NF-κB pathway remains critically understudied, and the effects that alternative NF-κB activation has in specific cell populations is not well understood.[23]

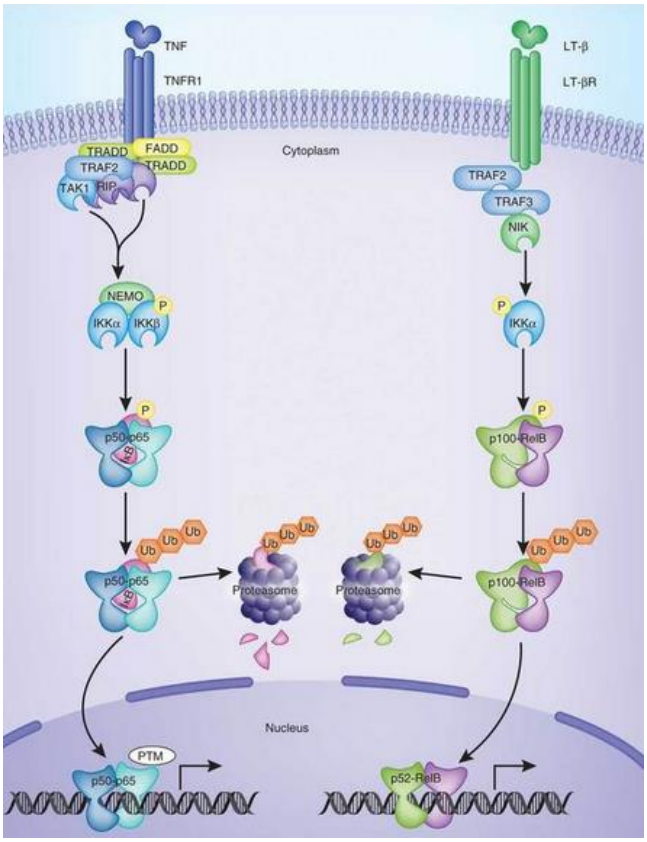

Figure 1.4: Classical (left) and alternative (right) pathways of NF-κB activation. The classical pathway is induced by most physiological NF-κB stimuli and is represented here by TNFR1 signaling. In the classical pathway, IκB-α is phosphorylated in an IKKβ and NEMO-dependent manner, which results in the nuclear translocation of mostly p65-containing heterodimers. In contrast, the alternative pathway, induced by certain TNF family cytokines, such as RANKL, involves IKKα-mediated phosphorylation of p100 associated with RelB, which leads to partial processing of p100 to p52 and the generation of transcriptionally active p52-RelB complexes. Figure adapted from source #3.[3]

It is well established that the classical NF-κB pathway controls the classical immune response of activated macrophages as well as many other non-immunogenic macrophage behaviors. The classical pathway is activated by binding of ligands to toll-like receptors at the cell surface, and by inflammatory cytokines such as lipopolysaccharide and tumor necrosis factor family members.[3] In response to these stimulatory signals, the classical NF-κB pathway causes macrophages to produce more inflammatory cytokines and recruit cells of the innate and adaptive immune system to the site of activation. The classical pathway also exhibits a low level of constitutive activation in mature macrophages. In contrast, alternative pathway function is far more selective and specific than classical NF-κB activation. Alternative activation of NF-κB in activated macrophages is poorly understood relative to the classical pathway but it is broadly known to play an important role in organogenesis and tissue architecture organization.[23, 24] The alternative pathway is not constitutively active in normal macrophages and is held in abeyance by sequestration and constant degradation of its activating kinase, NIK, by TRAF3.[25] Signal induced activation of protein kinases is usually mediated through post-translational modifications; however, NIK is unique in that its function is controlled by a steady level of expression. The expression level of NIK is normally kept low and bound by TRAF3, but is drastically

elevated in response to a specific alternative NF-κB activating signal.[26] In the tumor microenvironment signals such as TNF family members, inflammatory cytokines, and other cytokines such as M-CSF and IL-10 stimulate macrophages to undergo broad NF-κB activation. Though the NF-κB pathways are functioning normally, the activation of the pathways is deregulated by the tumor cells; the tissue remodeling effects of alternative NF-κB activation would be tumorigenic in this context.[9, 27]

The NF-κB pathways together produce complex pro- or anti-inflammatory and pro- or anti-tumorigenic effects. The interplay between the two pathways is made more confounding in that there is some unknown level of cross talk between the two, resulting in activation or depression of one or both pathways in different circumstances. This inherent complexity makes NF-κB a useful tool for tumor cells to utilize via local deregulation using tumor secreted cytokines, but it also makes NF-κB a very desirable target to manipulate in order to activate the innate cytotoxic, immunogenic properties of mature macrophages. One potential approach for manipulation of NF-κB in macrophages to create an anti-tumor environment is to selectively activate the strong immunogenic response associated with normal classical pathway activation while simultaneously turning off the tissue remodeling effects associated with the alternative pathway. This method of turning off one pathway while activating the other would rob the tumor of its supportive macrophages, reduce the complexity of NF-κB cross talk in TAMs, and create an anti-tumor phenotype in resident macrophages. Ideally, these macrophages would be capable of direct phagocytosis of tumor cell related materials (tumor cells and microvesicles), release apoptotic signals, and recruit $CD8^+$ T-cells and other activated immune cells to the tumor microenvironment.

Manipulating NF-κB by transfecting macrophages with siRNA

NF-κB is a promising therapeutic target for manipulation of macrophage phenotype to induce anti-tumor behavior. However, a broad, untargeted manipulation of NF-κB would likely result in negative side effects and would not produce the precise activity required to induce an anti-tumor phenotype in macrophages. In order to deliver a therapeutic agent to this specific cell population, a targeted delivery method would be ideal.[28] In a current collaboration between the Giorgio, Yull, and Duvall laboratories, a

novel mannosylated nanoparticle has been developed. This particle targets the mannose receptor found on the surface of macrophages and upregulated in TAMs.[12, 29] The core of the particle is created by RAFT polymerization of BME, PAA, and DMAEMA to create a hydrophobic, terpolymer with tunable endosomal escape properties.[30, 31] Next, a polycationic DMAEMA block is added by RAFT polymerization to add the capability to condense polyanionic therapeutics onto the particle. Finally, an AzEMA block is polymerized onto the diblock polymer to form a triblock polymer terminated in an AzEMA block to support further functionalization. In order to create a mannose functionalized polymer, click chemistry is performed with alkyne –functionalized mannose to attach a mannose moiety to the end of the polymer.[13, 32] The completed polymer assembles into positively charged micelles when reconstituted in an aqueous solution, forming mannosylated nanoparticles (MnNP; Figure 1.5).

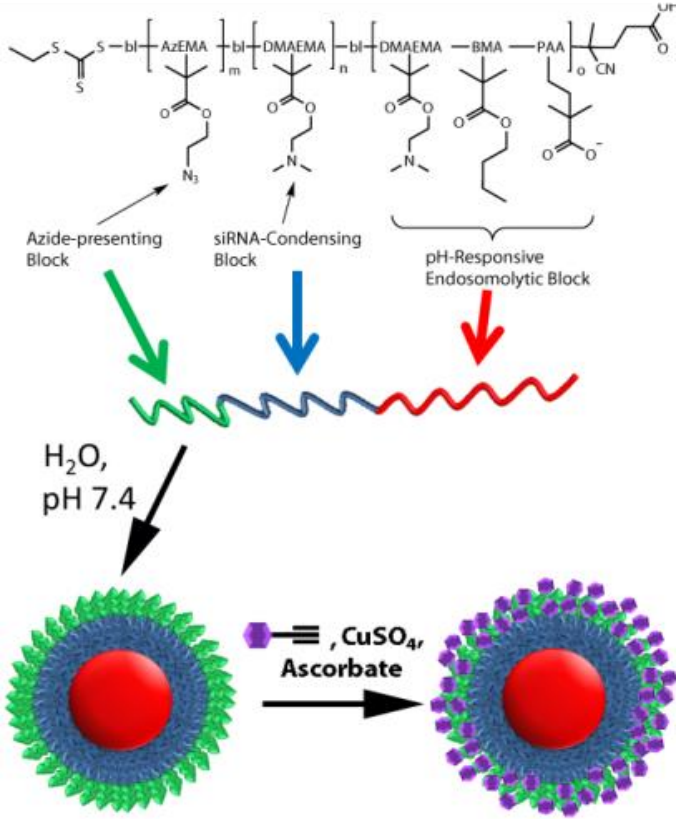

Figure 1.5: Schematic representation of the endosomal-escape polymeric nanoparticles for mannose receptor-targeted delivery of siRNA.

siRNAs are short therapeutically active RNA strands that knock down the translational activities of specific mRNAs without significant off-target side effects.[33] siRNA knocks down levels of target proteins by binding to complementary mRNA strands, resulting in the degradation and/or inactivation of the target mRNA strand.[10] Far from being just a laboratory tool, siRNA has been shown to have clinical translational potential, and targeted delivery of therapeutic siRNA has been accomplished in humans.[11, 34] As a therapeutic agent with tunable activity and high specificity, this polyanion is well suited for incorporation into MnNP to be used to target and treat TAMs *in vivo*.

Furthermore, because mature macrophages are largely non-proliferative, delivered siRNA would not be diluted by cell division. There are many commercial transfection agents, such as Lipofectamine, with the ability to deliver siRNA to cells *in vitro*; however, MnNP have a more neutral surface charge, indicating potential *in vivo* biocompatibility. Macrophages are notoriously difficult to transfect, but this vehicle is uniquely suited for use in experiments targeting TAMs in *in vivo* models of cancer and delivering NF-κB modulating siRNA sequences.

Hypothesis and Specific Aims

The hypothesis of this work is that mannosylated, endosomal escape nanoparticles can be used to target tumor associated macrophages and deliver siRNA to manipulate NF-κB activation in macrophages with the intent of activating tumor immunity. This work is a collaborative effort between multiple research groups with expertise in the areas of nanotechnology, polymer chemistry, molecular biology, mouse models of cancer, and cancer immunology. The combined effort of these groups has resulted in the completion of collaborative research that could not be performed by any single group alone.

Aim #1: Develop an efficacious *in vitro* protocol for transfecting macrophages with siRNA using MnNP and screen NF-κB specific siRNA sequences.

Aim #2: Determine optimum targets in the NF-κB pathways and analyze the potential therapeutic effects of knocking down those targets with MnNP-delivered siRNA.

Aim #3: Demonstrate the targeted delivery of nucleotides by MnNP in an *in vivo* mouse model of a solid cancer with a significant TAM population.

CHAPTER 2

In vitro optimization of macrophage transfection using commercial and nanoparticle transfection agents

Introduction

Recent decades have bought great advances in gene therapy technologies, specifically the emergence of siRNA. siRNAs can be used to inhibit the translation of specific mRNAs without significant off-target side effects by RNA interference (RNAi).[33] RNAi results in loss of target protein expression by siRNA binding to complementary mRNA strands, leading to mRNA degradation.[10] The clinical translation potential of siRNA has been demonstrated by the targeted delivery of therapeutic siRNA in humans.[11, 34] Another advantage of siRNA is that the degree of knockdown can be tuned to varying degrees of specificity, potency, duration by taking advantage of the transient nature of siRNA inhibition.[35] One of the current obstacles therapeutic siRNA faces is the delivery of active siRNA to specific cells types. Free siRNA is rapidly degraded *in vivo* by circulating RNases In addition, the strong polyanionic charge and significant molecular mass limits cellular entry of unformulated siRNA. An siRNA delivery vehicle that provides preferential localization to particular tissues and/or target cell types as well as superior siRNA protection and cellular entry is required for optimal and spatially specific RNAi.

Targeted nanoparticles have been used in clinical trials of siRNA therapeutics as a delivery device to reach specific cell populations.[31] The generation of a charge-neutral or near-neutral surface of a nanoparticle carrier of siRNA improves biocompatibility, as well as allowing for the potential attachment of a targeting ligand to the surface of the particle, improving cellular specificity. To address this, we have developed and characterized a tri-block polymer nanoparticle that specifically targets TAMs for siRNA delivery. The particle is designed such that the pH responsive core disrupts the endosomal compartment upon cellular uptake, rupturing the organelle as the internal pH drops and releasing the functional siRNA

into the cytoplasm.[36-38] One advantage of this core block design is its self-assembly into particles in an aqueous solution due to its tunable hydrophobicity.[39] The second block is a poly(DMAEMA) polymer with a polycationic charge that condenses polyanionic oligonucleotides within the particle and serves to carry and protect siRNA for delivery to a target cell. A distal, azide-presenting block serves as a modular platform for further functionalization with targeting ligands or other biomolecules of interest and represents novelty in the nanoparticle synthesis scheme relative to our previous work.

Using 'click' chemistry, we have functionalized the surface of these nanoparticles with a mannose ligand (MnNP) to specifically target TAMs via the mannose receptor, CD206.[13] The mannose receptor is highly specific to mature macrophages and has been shown previously to be upregulated on the surface of TAMs.[12, 29, 40] The mannose receptor is an endosomal, pattern recognition receptor which, when present at high levels, participates in suppression of the classical immune response.[40, 41] We have shown previously that uptake of these mannosylated endosomal escape nanoparticles (MnNP) by macrophages is mannose dependent and that uptake of MnNP is enhanced in macrophages compared to uptake of untargeted, hydroxyl capped nanoparticles (OHNP).[13] MnNPs are systematically designed to condense and shield siRNA in the interior of the particle for optimal systemic transport, enter the tumor vasculature via the enhanced permeability and retention (EPR) effect, specifically target TAMs in the tumor microenvironment, and escape the low pH late endosome to deliver functional siRNA into the cytoplasm.

Materials and Methods

Cell culture. Unless otherwise stated, all primary cells and cell lines used in this study were maintained in DMEM (Corning, MT-10-13-CV) with the addition of 10% (vol:vol) FBS and 1% Pen Strep (Gibco) at 37°C in a 5% CO_2 humidified atmosphere.

Bone marrow derived macrophage (BMDM) culture. Bone marrow derived macrophages (BMDMs) were made by harvesting bone marrow from wild type and NGL mice on an FVB background. Cells from NGL mice produce luciferase and GFP as a readout of total NF-κB activation. The media for

these cells contained 10% (vol:vol) FBS, 1% Pen Strep (Gibco), 5% heat inactivated horse serum (Gibco), 1% MEM non-essential amino acid mixtue (Sigma), 50 µM 2-mercaptoethanol (Sigma), and was supplemented with media from L-129 fibroblasts as a source of M-CSF.[42] The bone marrow was cultured for 6 days in the M-CSF supplemented media and the resultant BMDMs were scraped from their plates and re-plated as necessary for further experiments.

Luciferase activity readout in reporter cells. For cells producing luciferase as a readout of total NF-κB activation, the Promega luciferase assay system with reporter lysis buffer was used to measure luciferase activity. Plated cells were frozen in 1x reporter lysis buffer, then went through a thaw-freeze-thaw cycle before being scraped from the plates, and centrifuged at 13,000 rpm for 4 minutes. 20 µl of the supernatant was added to 100 µl of the luciferin substrate, and the resulting luminescence was counted to determine luciferase activity.

TNF-α stimulation of cultured macrophages. In order to induce NF-κB activation in macrophages, NGL BMDMs were stimulated with 0.01-1000 ng/ml of TNF-α (Peprotech) for 6 hours. After 6 hours, NF-κB activation was assessed by luciferase assay. For subsequent experiments including TNF-α stimulation, 10 ng/ml concentrations were used. Because transfection of cells can be improved in some cases by utilization of serum-free media, the possibility of coincident transfection and stimulation was investigated by stimulating NGL BMDMs with TNF-α (10 ng/ml, 6 hrs) in serum-free conditions. Stimulation efficacy was assessed by luciferase assay.

NF-κB activation in macrophages with tumor treated media. The HLL macrophage cell line is a line of immortalized macrophages that produces luciferase as a readout of total NF-κB activation. HLL macrophages were plated in the wells of 12-well plates at a density of 300,000 cells/well (approximately 80,000 cells/cm^2). Tumor cell treated media was produced by culturing PYG 129 polyoma tumor cells, L129 polyoma tumor cells, and ID8 ovarian tumor cells in media for 3 days.[43-45] The HLL macrophages were exposed to the tumor cell treated media for 1, 6, and 18 hours. As a control for different methods of NF-κB-related macrophage stimulation, cells were also stimulated with TNF-α (10 ng/ml) (Peprotech) or

lipopolysaccharide (LPS, 100 ng/ml) (Sigma) and interferon-γ (IFN-γ, 20 ng/ml) (Peprotech). After incubation with the tumor cell treated media, the HLL macrophages were analyzed for total NF-κB activation by measuring luciferase activity.

Luciferase knockdown in NGL reporter BMDMs with siRNA delivered by HiPerFect. NGL BMDMs were plated in 12-well plates at a density of 300,000 cells per well (approximately 80,000 cells/cm^2). Anti-luciferase siRNA (50 μM stock solution) (Life Technologies, AM4629) was added to 3, 6, 10, and 20 ul of HiPerFect (Qiagen) and allowed to form complexes for 1 hour. After complex formation, siRNA-HiPerFect complexes were added to the cell culture media for a final siRNA concentration of 10 nM. The cells were transfected for 24 hours. To induce NF-κB activity and luciferase production, the cells were stimulated for 6 hours with TNF-α (10 mg/ml) and luciferase activity was measured.

Assessment of siRNA mediated NF-κB knockdown using anti-IKKβ and anti-p52/p100 siRNA. NGL BMDMs were plated in 12-well plates at a density of 300,000 cells per well (approximately 80,000 cells/cm^2). In order to assess the efficacy of the purchased siRNA sequences (Life Technologies), anti-IKKβ siRNA (s68173) and anti-p52/p100 siRNA (s70545) were complexed with HiPerFect for a total dose of 10 nM siRNA, 20 μl HiPerFect per well. A scrambled siRNA sequence (4390846) was used as a negative control for siRNA activity and unloaded HiPerFect was used (20 μl per well) as control for macrophage stimulation by the transfection agent. Luciferase siRNA was delivered as a positive control. The cells were transfected for 24 hours. The last 6 hours of transfection included concurrent stimulation with TNF-α. Total NF-κB knockdown was assessed by luciferase assay.

Fabrication of nucleotide loaded MnNP. MnNP were fabricated as previously described.[13] Briefly: the core of the particle is created by RAFT polymerization of butyl methacrylate (BMA), 2-propylacrylic acid (PAA), and 2-(Dimethylamino)ethyl methacrylate (DMAEMA) to create a hydrophobic, terpolymer with tunable endosomal escape properties. Next, a polycationic DMAEMA block is added by RAFT polymerization to add the capability to condense polyanionic therapeutics onto the particle. Finally, a 2-Azidoethyl methacrylate (AzEMA) block is polymerized onto the diblock polymer to form a triblock

polymer terminated in an AzEMA block to support further functionalization. In order to create a mannose functionalized polymer, click chemistry is performed with alkyne –functionalized mannose to attach a mannose moiety to the end of the polymer. The completed polymer assembles into positively charged micelles when reconstituted in an aqueous solution, forming mannosylated nanoparticles.

For experiments using MnNP to deliver siRNA or short, fluorescently labeled DNA strands, MnNP polymer was reconstituted in sterile PBS at a concentration of 4 mg/ml and sonicated for 10 minutes. The MnNP in aqueous solution were used immediately or stored in aliquots at -20 °C. For complexation with the MnNP, all nucleotides were diluted to 50 μM in sterile, nuclease-free water. In order to form MnNP-nucleotide complexes with the optimal N:P ratio as described in our previous work, the 4 mg/ml MnNP solution was combined with 50 μM nucleotide solution in a 2:1, vol:vol ratio (160 ng of MnNP polymer per pmol of siRNA). The nucleotides were allowed to complex with the MnNP for 1 hour at room temperature, then used in *in vivo* and *in vitro* experiments. Nucleotide loaded OHNP were also formulated using this protocol.

Protein level analysis of siRNA mediated knockdown using different transfection agents. In order to investigate the comparative knockdown efficacies of different transfection agents, knockdown of the luciferase reporter for NF-κB activity in NGL BMDMs was assessed by luciferase assay. To prepare samples for luciferase assay, NGL BMDMs were plated in 12-well plates at a density of 300,000 cells per well (approximately 80,000 cells/cm^2). Anti-luciferase siRNA was complexed with HiPerFect, Lipofectamine, OHNP, and MnNP and delivered to the cells at an siRNA concentration of 10 nM. The cells were transfected for 24 hours. The last 6 hours of transfection included concurrent stimulation with TNF-α. Total NF-κB knockdown was assessed by luciferase assay.

Analysis of nanoparticle transfection in serum-free conditions. To assess the effect of nanoparticle-delivered, siRNA mediated knockdown in serum-free conditions NGL BMDMs were plated in 12-well plates at a density of 300,000 cells per well (approximately 80,000 cells/cm^2). Cells were transfected with anti-luciferase siRNA delivered by MnNP, OHNP, and Lipofectamine at 10 nM for 24

hours in serum-containing and serum-free media. The last 6 hours of transfection included concurrent stimulation with TNF-α. Total NF-κB knockdown was assessed by luciferase assay.

Nanoparticle uptake time course. Wild type BMDMs were cultured in normal media and media containing IL-4 (10 ng/ml) (Peprotech) for 72 hours. IL-4 stimulation has been reported to induce an M2-like phenotype in macrophages and increase mannose receptors on the cell surface.[46] The cells were then plated in 96-well plates at a density of 50,000 cells per well (approximately 350,000 cells/cm^2). A 21 base pair, Cy3-labled DNA sequence was purchased from Sigma for complexation with MnNP. The sequence was designed to have the same base pair order and charge characteristics as the scrambled siRNA sequence from Life Technologies. The Cy3_DNA were complexed with MnNP and OHNP and the complexes were delivered to the BMDMs. Cy3 fluorescence was measured at 0.5, 1, 3, 5, 10, and 18 hrs by washing the cells with PBS 3x and then measuring fluorescence with a Tecan Infinite M1000-Pro plate reader as a measurement of particle uptake. The dataset was analyzed using a two-factor analysis of variance (ANOVA) to determine if significant differences existed within the dataset. Post hoc analysis was performed using two-tailed T-tests for pairwise comparisons between selected groups. The probability for type I error in the post hoc analysis was reduced by minimizing the number of paired comparisons using *a priori* knowledge of the relationships between groups and selecting only the most pertinent comparisons.

siRNA sequence screen using Lipofectamine. Several siRNA sequences against NF-κB proteins were purchased from Life Technologies. The siRNA targets and serial numbers are summarized in Table 2.1. The siRNA were complexed with Lipofectamine and delivered to NGL BMDMs (12 well plates, 300,000 cells per well (approximately 80,000 cells/cm^2), 4 samples per conditions) for 24 hours at an siRNA concentration of 10 nM. The most successful sequences were then used at 50 nM and delivered to NGL BMDMs using both Lipofectamine and MnNP. For both studies, the effects of the siRNA on total NF-κB activity was assessed by luciferase assay following TNF-α stimulation of the cells.

Table 2.1: siRNA targets and serial numbers of siRNA sequences purchased from Life Technologies

siRNA Target	Serial Number
scrambled sequence	4390846
GAPDH	4390849
Luciferase	AM4629
IKKβ (A)	s68173
IKKβ (B)	s68174
IKKβ (C)	s68175
p52/p100 (A)	s70545
p52/p100 (B)	s70546
p52/p100 (C)	s70547
p65 (A)	s72857
p65 (B)	s72858
p65 (C)	s72859
IκBα	s70548

Rapid adhesion enrichment of TAMs. In order to enrich the TAM population from solid mammary and ovarian tumors, the tumors were removed and homogenized in cell culture media with Collagenase A (5 mg/ml, Roche) and DNaseI (5 mg/ml, Roche) for 2 hours. After 2 hours of incubation with gentle rocking, the homogenate was filtered through 70 micron filters and the cells were pelleted via centrifugation at 1000 g for 10 minutes. The pellet was then resuspended in 2 ml of ACK red blood cell lysis buffer (Gibco) for 2 minutes. The cell suspension was then diluted to 20 ml, pelleted, and the pellet resuspended in culture media. The tumor homogenate was then added to 6- or 12-well plates with 10 million, or 3 million cells per well, respectively. The homogenate was incubated in the welled plates for 45 minutes, and the non-adhered cells vigorously washed from the wells with PBS (3 washes), leaving the macrophages adhered to the plate at approximately 80-90% confluence.[47-51]

***In vitro* transfection of murine mammary PyMT TAMs.** Spontaneously arising murine mammary tumors were harvested at a palpable stage from 12 week old mice with a mammary epithelium targeted polyoma middle T oncogene (PyMT, FVB strain background).[52] TAMs were enriched into 12-well plates with a 45 minute, rapid-adhesion protocol. After the TAMs were isolated, they were transfected with FAM-labeled, scrambled siRNA (Ambion) for 2 and 6 hours using MnNP, alcohol-capped (non-targeted) endosomal escape nanoparticles (OHNP), or Lipofectamine. A control set of TAMs were incubated with free, FAM-labeled siRNA alone. After transfection, the cells were gently washed three times with sterile

PBS and fixed in 4% paraformaldehyde for 30 minutes at 4°C. FAM fluorescence was measured in each sample with a Tecan Infinite M1000-Pro plate reader as an indicator of siRNA delivery with 12 measurements per well in a filled circular pattern. The dataset was analyzed using a two-factor analysis of variance (ANOVA) to determine if significant differences existed within the dataset. Post hoc analysis was performed using two-tailed T-tests for pairwise comparisons between selected groups. The probability for type I error in the post hoc analysis was reduced by minimizing the number of paired comparisons using *a priori* knowledge of the relationships between groups and selecting only the most pertinent comparisons.

Results and Discussion

Bone marrow derived macrophages (BMDMs) as a model for TAMs. It has been reported that BMDMs are a viable, *in vitro* model for TAMs.[15] BMDMs are made from myeloid progenitor cells harvested from femoral bone marrow and matured in media supplemented with M-CSF. *In vivo,* M-CSF is a potent macrophage recruiting and maturation cytokine and is known to play a role in the recruitment of myeloid progenitors into tumors, and maturing these cells into macrophages.[17] In order to measure knockdown of NF-κB activity by siRNA, it is necessary to ensure that there is a measurable signal to knockdown. After 6 hours of incubation in TNF-α treated media, total NF-κB activity increased in dose dependent manner as measured by luciferase readout as a proxy measure of NF-κB activity (Figure 2.1A).

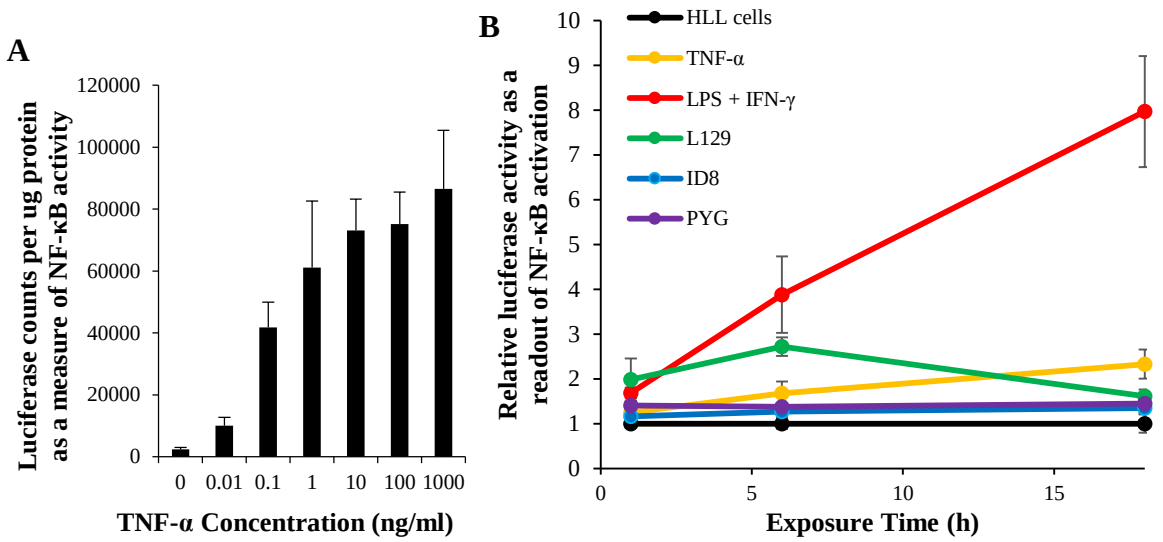

Figure 2.1: Activation of NF-κB in BMDMs by TNF-α and other stimulating agents. (A) Activation by TNF-α is dose dependent, with the dose response leveling off at approximately 10 ng/ml of TNF-α. (B) LPS in combination with IFN-γ induces strong NF-κB activation. This combination of molecules is known to activate the classical pathways. In contrast, activation with TNF-α, which activates both pathways, produces a lower amount of total NF-κB activity. Activation by TNF-α induces levels of activity similar to activation stimulated by tumor cell treated media from 3 tumor cell lines (L129 and PYG – murine mammary tumor cells, ID8 – murine ovarian tumor cells).

LPS treatment of the HLL cell line microphages induces a strong response as measured by luciferase assay as a readout of NF-κB activity, however, the results of treatment with TNF-α and tumor cell treated media is not as clear. Though it appears that TNF-α stimulates both pathways in a manner similar to stimulation with tumor treated media (Figure2.1B), it is possible that this observation is an artifact created by the low luciferase production of the HLL cells. There is some activation of HLL activity using TNF-α and tumor treated media, the magnitude of the response indicates that this particular cell line is not optimum for resolving small increases in NF-κB activation. Future studies should endeavor to reproduce these results in a different reporter macrophage, such as NGL BMDMs.

Screening NF-κB specific siRNA sequences for efficacy, using commercial transfection agents. In order to confirm that purchased siRNA could knock down NF-κB activity in macrophages, several sequences were screened in NGL BMDMs. MnNP fabrication, validation, and optimization had not finished, so commercial transfection agents were used to screen the siRNA sequences. Initially, HiPerFect was used as the commercial transfection agent. Product information for HiPerFect claims that it is a blend

of neutral and positively charged lipids and is able to transfect difficult to transfect cells such as macrophages with less toxicity than other commercial transfection agents. Upon the addition of the polyanionic nucleotide strand, the lipids form a micellular structure with the nucleotide encapsulated in the particle.

The amount of HiPerFect to be used for transfection was optimized by delivering anti-luciferase siRNA to stimulated NGL BMDMs and measuring knockdown of luciferase activity. 20 µl of HiPerFect per ml of media was found to produce the strongest knockdown using 10 nM siRNA (Figure 2.2A). These parameters were then used to test initial siRNA sequences for IKKβ in the classical NF-κB pathways and p100/p52 in the alternative pathway. IKKβ is an activating kinase for the classical pathway which phosphorylates the inhibitor protein bound to p50:p65 heterodimer. Knockdown of IKKβ should reduce activation of the classical pathway, mitigating the smoldering inflammation caused by TAMs. p100 is one of the transcriptionally active NF-κB proteins. A portion of this protein acts as the inhibitor of the alternative pathway and is degraded upon pathway activation. The resulting p52:RelB heterodimer is then free to undergo nuclear translocation. By knocking down p100/p52, alternative NF-κB signaling should decrease. It is my hypothesis that a decrease in alternative activation will decrease or remove the support that TAMs provide to tumor cells. Although these parameters resulted in 85% knockdown of luciferase activity using an anti-luciferase siRNA, knockdown of IKKβ resulted in 18% knockdown of total NF-κB activity and p100/p52 knockdown resulted in 40% knockdown of NF-κB activity. These percentages indicate some degree of success in decreasing NF-κB using the screened sequences, but the amount of HiPerFect required to achieve this knockdown rendered extended use of HiPerFect financially infeasible. Lower amounts of HiPerFect did not produce efficacious knockdown of NF-κB activity.

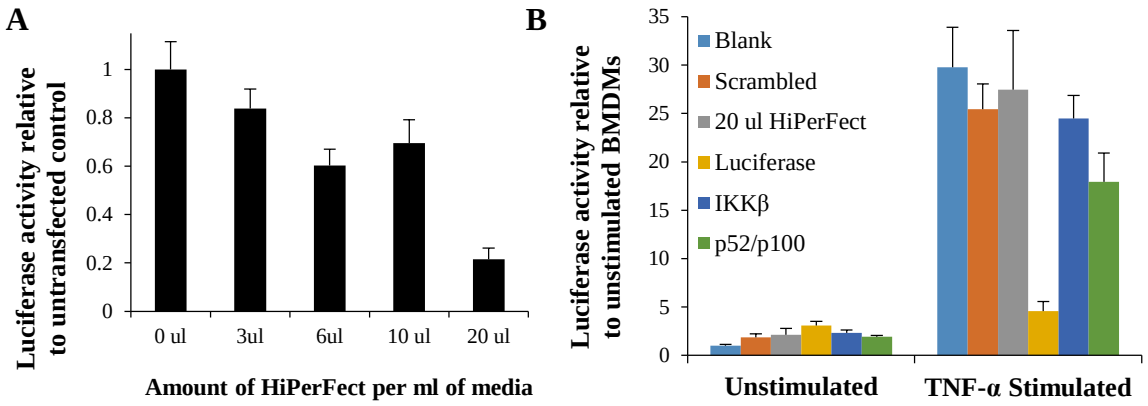

Figure 2.2: (A) Knockdown of luciferase in NGL BMDMs using HiPerFect with 10 nM anti-luciferase siRNA is dependent on the amount of HiPerFect used to deliver the siRNA. (B) Knockdown of total NF-κB activity by 10 nM siRNA with 20 ul/ml HiPerFect in NGL BMDMs. Knockdown of the model protein, luciferase, was satisfactory, but knockdown of total NF-κB by delivering siRNA for IKKβ and p52/p100 was less than desired.

Lipofectamine was selected as a more cost effective commercial transfection agent as an alternative to HiPerFect. The transfection ability of Lipofectamine was tested by performing a screen of siRNA sequences for IKKβ, p100/p52, and p65 (RelA). p65 is one of the transcriptionally activating proteins of the classical NF-κB pathway. It is normally bound in heterodimers with p50 and is activates hundreds of gene targets, including those associated with both strong and smoldering inflammation. Knockdown of p65 in TAMs should reduce smoldering inflammation in the tumor stroma. Furthermore, p65 is downstream from IKKβ, which has significant cross-talk with other intracellular pathways; therefore, targeting p65 should have fewer off-target effects than targeting IKKβ.

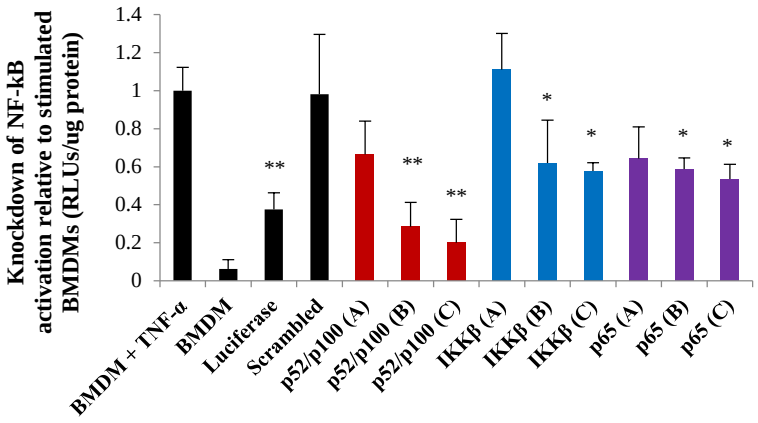

Figure 2.3: Knockdown of total NF-κB by Lipofectamine delivered siRNA sequences. Single factor ANOVA confirms significant differences within the data set ($P < 0.0001$). T-tests for significance compare TNF-α stimulated BMDMs to siRNA transfected BMDMs (control). * : $P \leq 0.05$, ** : $P \leq 0.01$.

Using Lipofectamine as the transfection agent, efficacious siRNA sequences were confirmed for the NF-κB related proteins shown in Figure 2.3. Transfection with IKKβ siRNA significantly reduced total NF-κB activity by approximately 40% for sequences B and C. Similar significant reduction in activation (40-45%) was measured following transfection with p65 siRNA sequences B and C. This level of knockdown in consistent with the strategy of delivering siRNA to reduce activation of a single pathway, which would leave the unaffected pathway free to normally respond to stimuli. It is interesting to note that knockdown of the alternative pathway with p52/p100 specific siRNA sequences (B and C) resulted in a 70-80% decrease in total NF-κB activity following TNF-α stimulation. From this result, it can be inferred that there is possibly a mechanism of direct or indirect cross-talk between the two pathways or that TNF-α stimulation of NF-κB activation in these cells was driven largely by the alternative pathway and the siRNA sequences for this pathway were very effective. These results indicate that knockdown of the classical pathway with siRNA may only affect that one pathway, while knockdown of the alternative pathway using siRNA may reduce activation of both pathways.

It is known that products of one NF-κB pathway can potentially activate the other; in particular, the TNF family of proteins.[3] It is possible that knocking down the alternative pathway is reducing the production of some cytokine that stimulates the classical pathway or that stimulates other pathways which

in turn activate classical NF-κB. Another possible explanation hinges on the fact that NF-κB activation can be accomplished with protein dimers other than p50:p65 and p52:RelB. It is possible that by knocking down p52, p52:p65 heterodimers, which could be activated by classical signaling, are also reduced. It is also possible that reduction of p52 activates a compensatory mechanism and results in more production of p105, which is degraded to p50; although there is currently no direct evidence for this mechanism. An increase in p50 could result in the formation of p50 homodimers, which are known to inhibit classical activation.[53]

Efficacy of MnNP as a transfection agent for macrophages. After the change was made from HiPerFect to Lipofectamine as the commercial transfection agent of choice, an experiment to compare all of the transfection agents at once was performed. Luciferase activity in stimulated NGL BMDMs was knocked down using 10 nM anti-luciferase siRNA delivered by both of the commercial agents and by targeted and untargeted nanoparticles. All of the transfection agents created significant knockdown of luciferase activity (Figure 2.4), with Lipofectamine producing the strongest knockdown. Importantly, this was the first test of the MnNP and OHNP delivery agents, both of which produced significant knockdown even though they were used following a protocol optimized for the commercial transfection agents.

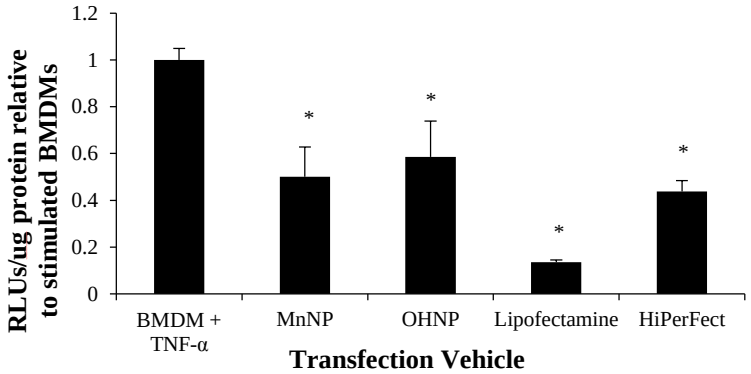

Figure 2.4: Knockdown of luciferase activity by anti-luciferase siRNA delivered by different transfection agents in TNF-α stimulated BMDMs. Dunnett's test for significance compare TNF-α stimulated BMDMs to siRNA transfected BMDMs. * : $P < 0.01$.

In order to improve transfection efficacy by MnNP, alterations to the commercial agent optimized protocol were investigated. In some cases, transfection under serum-free conditions can improve

transfection efficiency by removing the charged serum proteins that can potentially interact with the charged particle surface, reducing particle functionality or marking the particles for complement mediated immune clearance. Figure 2.5A shows that TNF-α stimulation of BMDMs, the model used for NF-κB activation in macrophages, is altered by serum-free conditions. Furthermore, transfection under serum-free conditions is less physiologically relevant than performing transfections in serum containing media. *In vivo* transfection of cells brings the transfection agent into contact with blood serum proteins, which is an important consideration when designing a therapeutically relevant nanoparticle transfection agent. However, as Figure 2.5B shows, MnNP (and OHNP) are designed such that the presence of serum proteins in the transfection media do not significantly reduce the knockdown effect mediated by the nanoparticle delivery device.

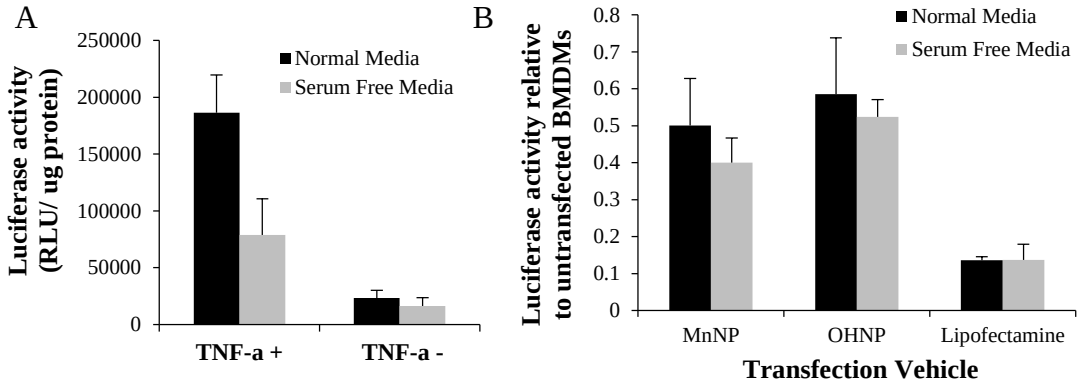

Figure 2.5: The effects of serum on BMDM stimulation and transfection. (A) Serum-free media decreases TNF-α activation of BMDMs. Knockdown of NF-κB in BMDMs is easier to measure given a strong initial signal. Any decrease in activation will increase the difficulty of measuring the knockdown effect of siRNA. Activation of NF-κB in serum-free conditions is sub-optimal for measuring the effects of siRNA. (B) The use of serum-free media does not significantly improve knockdown of luciferase by anti-luciferase siRNA delivered by nanoparticle transfection agents or Lipofectamine. Though in some cases, serum-free conditions can improve transfection, using serum-free conditions will not improve transfection of BMDMs by MnNP, OHNP, or Lipofectamine.

Once it was determined that serum-free conditions would not improve the transfection efficacy of MnNP, increasing the concentration of the delivered siRNA and MnNP delivery agent was investigated as a potential method of improving knockdown of NF-κB in macrophages. 50 nM siRNA was delivered to BMDMs for 24 hours by MnNP and Lipofectamine and knockdown of total NF-κB was analyzed following TNF-α stimulation. The most successful sequence for each protein from Figure 2.3 was delivered to the

BMDMs. As Figure 2.6 shows, MnNP-mediated, siRNA knockdown of total NF-κB activity was similar to Lipofectamine-mediated knockdown. Total NF-κB activity was significantly decreased upon MnNP delivery of siRNA sequences. For all future *in vitro* experiments utilizing MnNP, a 50 nM concentration of siRNA was used with a corresponding increase in MnNP concentration. Also noteworthy is that the average knockdown of total NF-κB activity by Lipofectamine-delivered siRNA was less than the knockdown from 10 nM siRNA. It is possible that this decrease in efficacy is due to an increase in cytotoxicity associated with increasing the amounts of the strongly positively charged lipids making up the Lipofectamine formulation.

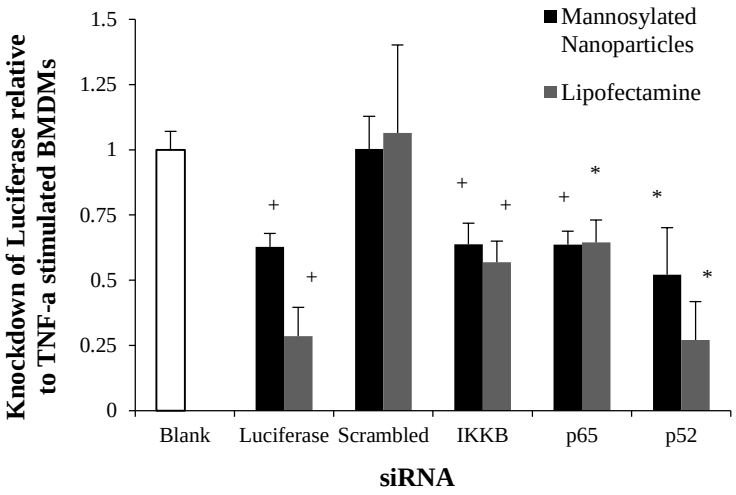

Figure 2.6: MnNP-delivered, 50 nM siRNA knockdown of total NF-κB activity is comparable to knockdown achieved by using Lipofectamine. In addition to exhibiting efficacious delivery and knockdown characteristics, MnNP are designed to be biocompatible both *in vitro* and *in vivo*. Dunnett's teats for significance compare TNF-α stimulated BMDMs (Blank, control) to siRNA transfected BMDMs. * : $P \leq 0.05$, + : $P \leq 0.01$

We have previously shown that uptake of MnNP is mannose dependent, and that uptake can be reduced by introducing free mannose during transfection, which competes with the MnNP for uptake by the macrophage mannose receptor.[13] To investigate the differences between untargeted, hydroxyl capped nanoparticles, OHNP, and MnNP, Cy3 labeled dsDNA was loaded into the particles and delivered to BMDMs for 18 hours. Two different populations of BMDMs were used: normal BMDMs and BMDMs stimulated with IL-4 to increase mannose receptor production.[46] Particle uptake by BMDMs was measured

at various time points by measuring Cy3 fluorescence in the BMDMs. In IL-4 stimulated macrophages, uptake of MnNP is significantly increased as compared to uptake of MnNP in unstimulated macrophages (Figure 2.7). Uptake of OHNP is not significantly different between the two groups of cells. This result indicates that the mannose ligand on the surface of the MnNP is mediating enhanced uptake that is specific for macrophages that have undergone phenotypic differentiation by IL-4.

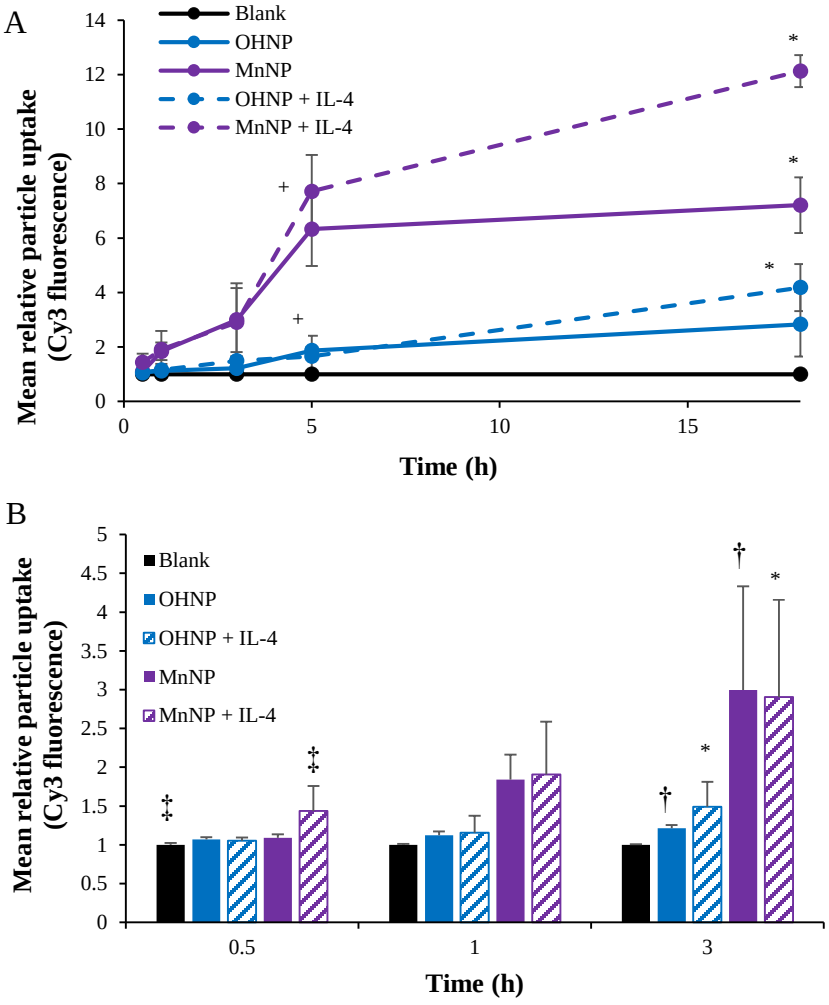

Figure 2.7: Nanoparticle uptake time course in IL-4 stimulated and unstimulated BMDMs. Analysis of variance indicates significant differences within the data set ($P<0.001$) (A) Uptake of MnNP in IL-4 stimulated BMDMs was significantly greater than uptake in unstimulated BMDMs after 18 hrs. Uptake of MnNP under both conditions was significantly greater than uptake of OHNP after 5 and 18 hours. (B) Earlier time points of nanoparticle uptake are highlighted. Uptake of MnNP occurs as early as 30 minutes after administration. Uptake of MnNP is significantly greater than uptake of OHNP after 1 hour. T-tests for significant differences in group averages were performed between multiple experimental groups. † , ‡ : $P \leq 0.05$, * or + : $P \leq 0.001$.

Although IL-4 stimulated BMDMs are reported to have increased mannose receptor production, unstimulated BMDMs also express this receptor at their surface. This explains why, even at earlier time points, MnNP uptake is enhanced relative to OHNP uptake in both IL-4 stimulated and unstimulated BMDMs. Significant uptake of MnNP occurs as early as 30 minutes after administration to IL-4 stimulated BMDMs. This rapid uptake is consistent with endosomal uptake of the particles, in this case mediated by the mannose receptor. These results also indicate that the particles can be taken up to some small extent in a non-specific manner. It is likely that some particles are phagocytized by the macrophages or taken up via other, non-specific endosomal pathways.

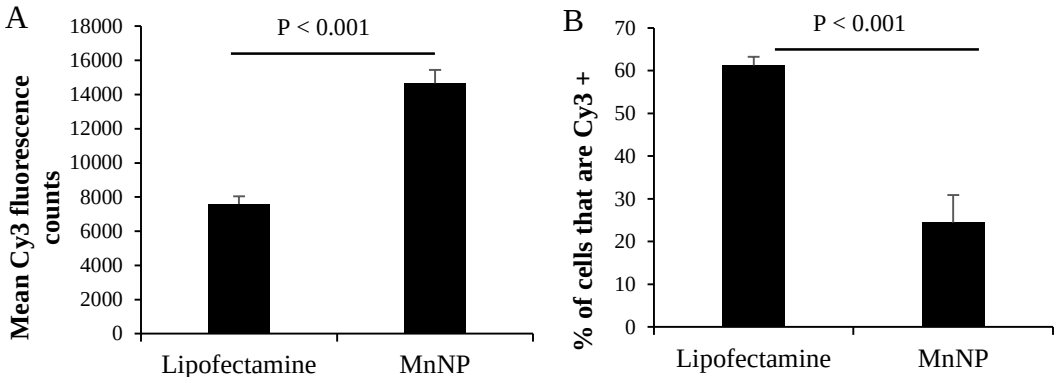

Figure 2.8: (A) Transfection of BMDMs with MnNP resulted in significantly more uptake of Cy3 labeled nucleotide than transfection with Lipofectamine after 20 hours. (B) MnNP transfect a smaller subset of cells than Lipofectamine. Lipofectamine transfects a larger population of cells with Cy3 labeled nucleotide, but the total fluorescence delivered is approximately half that delivered by MnNP.

A final experiment investigating the mechanism of MnNP delivery to macrophages compared 20 hour MnNP delivery to Lipofectamine delivery. Both transfection agents were labeled with Cy3_dsDNA. After 20 hrs of incubation, Cy3 fluorescence was measured as an indicator of particle uptake and the percent of Cy3 positive cells was determined from fluorescent and bright-field images of the cells. Figure 2.8A shows that transfection with MnNP resulted in significantly more uptake of Cy3 labeled nucleotide than transfection with Lipofectamine. Furthermore, Lipofectamine transfects a larger population of cells with Cy3 labeled nucleotide, but the total fluorescence delivered is approximately half that delivered by MnNP. Compared to Lipofectamine, MnNP strongly transfect a smaller subset of macrophages. This is consistent

with the mechanism of MnNP transfection being a more targeted delivery to cells expressing the corresponding surface receptor. This combined with our previous report that uptake of MnNP is mannose dependent indicates that MnNP are targeting a subset of macrophages with greater amounts of mannose receptor. This result highlights the potential for MnNP to target the appropriate subset of macrophages *in vivo*. Macrophages (and TAMs) with a tissue remodeling/immunoinhibitory phenotype have increased mannose receptor production. This effect is so pronounced that the presence of high levels of mannose receptor in macrophages is a commonly used indicator for this macrophage phenotype.

MnNPs enhance *in vitro* delivery of fluorescently labeled siRNA to TAMs *ex vivo*. Spontaneously arising murine mammary tumors were harvested from 12 week old mice containing a mammary epithelium targeted polyoma middle T oncogene (PyMT).[52] The tumors were dissociated and the resident TAMs from the tumor homogenate were enriched.[47-51] TAMs were transfected with FAM-labeled siRNA for 2 or 6 hours with either MnNP, hydroxyl-capped (non-targeted) endosomal escape nanoparticles (OHNP), or Lipofectamine (Figure 2.9).

After 6 hours of transfection, TAMs exposed to MnNP-siRNA_FAM had significantly higher FAM fluorescence than TAMs transfected with Lipofectamine (1.6-fold increase in FAM fluorescence vs 1.25-fold increase). Furthermore, fluorescence measured in TAMs transfected with the non-targeted OHNP was not significantly different than the fluorescence measured in TAMs transfected with the highly cationic Lipofectamine (also possessing no specificity for TAMs). For all samples, siRNA delivery increased from 2 to 6 hours, with the greatest increase occurring in the MnNP transfected samples. The rate of MnNP uptake by the TAMs is also increased at the 2 hour time point compared to the untargeted transfection agents. I observed a burst effect in delivery during the first few hours in the MnNP transfected samples indicating rapid, mannose-mediate uptake. Without the aid of transfection complexes, a small amount of free siRNA is taken up by the TAMs. This is likely due to phagocytosis of the siRNA molecules by the macrophages following binding of serum proteins to the siRNA. It is important to note that while unmodified siRNA may be taken up by cells in a non-specific manner both *in vitro* and *in vivo*, siRNA

delivered in this fashion exhibits little to no activity. The transfection efficacy of the untargeted nucleotide, OHNP and Lipofectamine, are similar. Previously, we have demonstrated enhanced siRNA delivery to murine BMDMs *ex vivo* by MnNPs to be mannose dependent. Results of this study, with TAMs, are consistent with earlier findings confirming MnNP recognition by CD206 in BMDMs.[13]

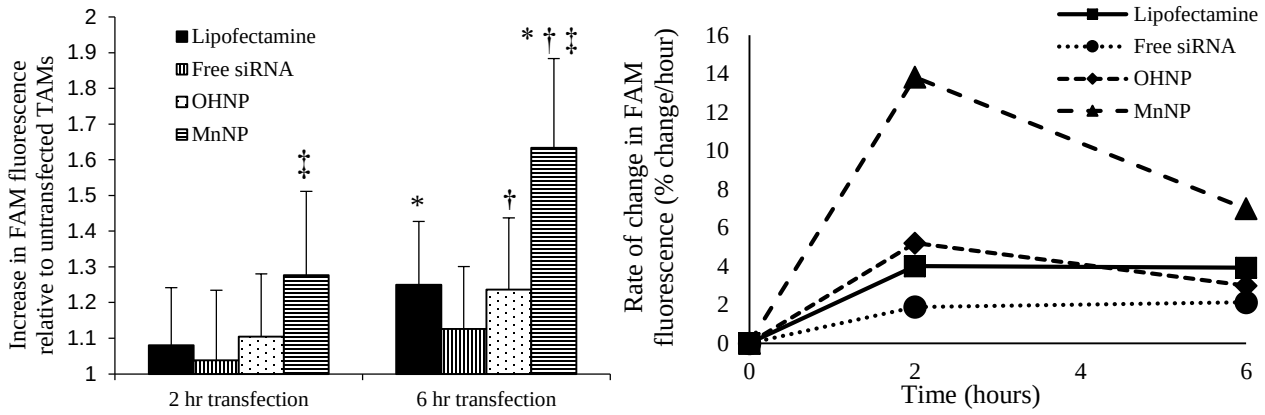

Figure 2.9: In vitro transfection of TAMs isolated from murine mammary PyMT tumors with MnNP results in greater uptake of FAM labeled siRNA as compared to other transfection agents. Analysis of variance indicates the presence of significant differences within the dataset ($P<0.001$). MnNP creates a significantly greater increase in FAM fluorescence in the TAMs from the 2 hr to the 6 hr time point as compared to Lipofectamine or the non-targeted OHNP (*,†, ‡: $P < 0.05$) and the high rate of change of FAM fluorescence in these cells indicates a rapid burst effect in delivery using MnNP. The two non-targeted agents have similar delivery efficacies.

Conclusions

Mannosylated nanoparticles are capable of delivering functional siRNA to macrophages *in vitro*. While initial experiments used HiPerFect as a commercially available comparison for MnNP, it was later deemed unfeasible for continued use and Lipofectamine was chosen as a replacement. MnNP are capable of delivering functional siRNA for NF-κB proteins to macrophages, and the total reduction of NF-κB activity is comparable to that achieved with Lipofectamine delivery. The MnNP have the added trait of being specifically designed to be compatible with *in vivo* use. Investigations into the practical aspects of using MnNP to transfect macrophages resulted in the conclusion that the particles can be used effectively in serum containing media and that knockdown of NF-κB activity is best observed under pathway

activating conditions, such as TNF-α stimulation of the macrophages: the effect of siRNA is more evident when there is a strong signal to knockdown.

MnNP are taken up to a greater degree in macrophages with increased mannose receptor presence (induced by IL-4 stimulation) compared to wild type macrophages. The enhanced uptake of MnNP by IL-4 stimulated macrophages compliments our previous results indicating that MnNP uptake is mannose dependent. Furthermore, uptake of untargeted particles by IL-4 stimulated macrophages was not different from uptake of the same particles by wildtype macrophages. There is greater overall uptake of the MnNP than the OHNP, and uptake of MnNP occurs at earlier time points. A comparison of MnNP and Lipofectamine revealed that MnNP strongly transfect a small population of macrophages in the BMDM population, while Lipofectamine moderately transfects a larger population of BMDMs. Comparisons between MnNP and non-specific transfection agents were confirmed in an enriched TAM population. Significant uptake of MnNP in TAMs occurs earlier than non-specific agents and there is a burst effect in the rate of change of particle uptake that is only seen with MnNP transfection at early time points.

CHAPTER 3

In vitro manipulation of NF-κB in macrophages using MnNP delivered siRNA results in a potentially anti-tumor phenotype

Introduction

Immunotherapy as a treatment for cancer is seeing a resurgence. Many therapeutic strategies, such as adoptive T-cell transfer for prostate cancer, focus on activating or enhancing adaptive immunity against cancer cells.[54, 55] However, cells of the innate immune system are also an attractive target. Tumor associated macrophages (TAMs) have been implicated as one of the most prevalent and impactful types of immune cells in the tumor related stroma.[1, 2, 56] In most cases, the genetic material of TAMs is stable and free of mutations, but interactions between the tumor cells and the resident or infiltrating macrophage population have caused the macrophages to adopt a phenotype characterized by the constant production of low levels of inflammatory cytokines.[15] This produces a state of smoldering inflammation in the tumor and surrounding tissue. This type of inflammation is not strong enough to induce apoptosis or other mechanisms of cell death in the tumor cells, but is significant enough to cause survivable DNA damage in the tumor cells' genetic material as well as activate survival signals in the nearby cells.[7, 20] Paradoxically, TAMs also produce immunosuppressive cytokines, such as IL-10, which suppress the ability of resident immune cells to act against the invading tumor cells and prevents the recruitment of $CD8^+$ T-cells, NK cells, and other cytotoxic or pro-inflammatory immune cells.[57-59] Furthermore, TAMs produce growth factors and can degrade surrounding connective tissue and induce angiogenesis, allowing the primary tumor to grow.[52, 60, 61] Finally, TAMs participate in the metastatic process by creating pathways which aid tumor cell intravasation.[4, 18]

It has been reported that the tumorigenic and metastatic effects generated by TAMs can be reduced or removed by ablating macrophages with liposomal clodronate in mouse models of human cancer.[18]

Though TAMs have adopted a pro-tumor phenotype, as macrophages they have the potential to produce cytotoxic levels of inflammation, lyse surrounding cells, and coordinate an immune response from cells of the innate and adaptive immune system.[42, 43, 62, 63] The ability to recapitulate these cytotoxic and immunostimulatory functions in TAMs, creating an anti-tumor phenotype, would be a powerful therapeutic tool for treating tumors and metastases known to have a significant macrophage population. This anti-tumor phenotype could be produced by strategically manipulating the NF-κB pathways in TAMs. The NF-κB pathways are potent controllers of macrophage phenotype and regulate many of the inflammatory and trophic functions of macrophages.[64-66]

Although the classical NF-κB pathway is a constitutively active survival pathway, strong, acute activation of the classical pathway by inflammatory molecules such as LPS or TNF-α creates a pro-inflammatory phenotype in macrophages.[67-69] In contrast, the alternative NF-κB pathway is activated by a narrower set of molecules; primarily the tumor necrosis factor family of cytokines (RANKL, CD40L, TWEAK, TNF-α).[23] Activation of the alternative NF-κB pathway in macrophages has been shown to be necessary for the formation of lymph nodes and Peyer's patches. Mice without functioning alternative NF-κB pathways in macrophages also have disorganized splenic and thymic architecture.[70, 71] The mechanisms and down-stream effects of NF-κB activity in TAMs is not completely understood, but the current understanding of the ultimate effect of NF-κB activation in solid tumors is that it contributes to both smoldering inflammation and to tumor-sustaining effects.

In the past, the prevailing wisdom regarding NF-κB activity in tumors has been that activation of these two pathways in the context of primary or metastatic tumors creates strong pro-tumor effects.[44] However, given the current understanding of the effects of NF-κB activation in specific cell populations, this theory is too generalized. Recent work in mice with activatable classical NF-κB signaling in macrophages has shown that strategic activation of the classical pathway profoundly reduces metastatic tumor burden in a tail-vein injected mouse model of metastatic breast cancer. This reduction in lung metastases could be explained by the increase in mRNA for inflammatory cytokines and T-cell recruitment

cytokine, CXCL9, and a decrease in mRNA for molecules associated with tissue remodeling and suppression of immune activity.[43] This highlights the therapeutic potential of strategically activating NF-κB in TAMs in order to activate an acute, strong inflammatory phenotype.

Ideally, a strategy for activating anti-tumor immunity in TAMs would decrease the supportive effects these cells have on the tumor, and simultaneously activate a potent immune response to the tumor cells, leveraging both the innate and adaptive immune systems. A potential mechanism for creating this effect is knocking down alternative NF-κB activation and increasing classical NF-κB activation in TAMs. The therapeutic agent used to achieve this effect should be highly specific for the target NF-κB components and should create a strong, targeted, transient effect: it would be counter-productive to create weak inflammation or permanent, strong inflammation at the site of the tumor, or to cause systemic inflammation.

I have screened several NF-κB specific siRNA sequences using both the commercial transfection agent, Lipofectamine, as well as MnNP. Initially, my strategy was to knock down both classical and alternative activation in order to reduce pro-tumor TAM effects. During the course of the study, I discovered that siRNA against the inhibitor protein of the classical pathway activates the classical pathway, potentially inducing a pro-inflammatory, immunogenic phenotype in the transfected macrophages. Here I detail my work validating the efficacy of MnNP as transfection agents for delivering siRNA designed to knockdown IκBα, which I hypothesize will activate classical NF-κB signaling. Finally, I investigate the potential therapeutic efficacy of using MnNP-delivered siRNA to activate the classical NF-κB pathway or to knock down the alternative NF-κB pathway in macrophages.

Materials and Methods

Cell culture. Unless otherwise stated, all primary cells and cell lines used in this study were maintained in DMEM (Corning, MT-10-13-CV) with the addition of 10% (vol:vol) FBS and 1% Pen Strep (Gibco) at 37°C in a 5% CO_2 humidified atmosphere.

Effect of IκBα siRNA on total NF-κB activation in macrophages. To investigate the possibility of activating the classical NF-κB pathway by knocking down the inhibitor of the classical pathway, IκBα, siRNA against IκBα was delivered to NGL BMDMs in 12 well plates at 50 nM for 24 hours using MnNP. MnNP were fabricated as described in Ch. 2. Free siRNA and empty MnNP were also delivered separately as controls. Total NF-κB activation was assessed at various time points by luciferase assay.

qRT-PCR of BMDMs transfected with p52/p100 and IκBα siRNA. Wild type BMDMs were plated in 6-well plates at a density of 2,000,000 cells per well (approximately 210,000 cells/cm^2). Each sample was taken from a different mouse, for a total of 3 biological replicates, with 3 experimental replicates per biological replicate. The cells were transfected using MnNP for 24 hours with IκBα, p52/p100, or scrambled siRNA, with and without TNF-α stimulation. After transfection, mRNA was collected from the cells for qRT-PCR.

Preparation of mRNA for qRT-PCR. mRNA was extracted from cells using Qiagen's RNeasy kit and DNA was removed from the samples using Life Technologies' DNA-free kit. cDNA was prepared from the isolated mRNA using dNTPs from Roche and random hexamers and superscript II reverse transcriptase from Life Technologies. qRT-PCR was performed with SYBR green real-time PCR master mix (Life Technologies) using Applied Biosystems' Step One Plus real-time PCR systems hardware and software. The Step One Plus software was used to automatically calculate optimized baseline and threshold values. Differences in cDNA levels were calculated using the ΔΔCt method with GAPDH as an internal control. The sequences used for qRT-PCR are summarized in Table 3.1.

Table 3.1: qRT-PCR primer sequences

Gene	Forward Sequence (5'-3')	Reverse Sequence (5'-3')
GAPDH	TGAGGACCAGGTTGTCTCCT	CCCTGTTGCTGTAGCCGTAAT
IκBα	TGAAGGACGAGGAGTACGAGC	TTCGTGGATGATTGCCAAGTG
p100	GCTTCTCAGCTTTCCTTCGAGCTA	GCAAATAAACTTCGTCTCCACCGC
IKKβ	GCTGGAGCAGAGAAATGTCAGAGT	CTCAGGAACAATCAAAGCGTGCAG
CXCL9	GTGGTGAAATGGAAAGATCAGGGC	AAGAGAGAAATGGGTTCCCTGGAG
IL-10	ACCTGCTCCACTGCCTTGCT	GGTTGCCAAGCCTTATCGGA
CD206	CAAGGAAGGTTGGCATTTGT	CCTTTCAGTCCTTTGCAAGC
CCL3	TGCCCTTGCTGTTCTTCTCT	GATGAATTGGCGTGGAATCT

Statistical analysis. Paired comparisons were made using a two-tailed T-test to determine significant differences between samples. For figure 3.4, multiple comparisons were made by first performing single factor ANOVA to confirm significant differences within the groups, then *post hoc* analysis was performed using two-tailed T-tests, for six total comparisons (30% chance for type I error).

Results and Discussion

Target protein selection for strategic manipulation of NF-κB to produce therapeutically relevant changes in TAM phenotype. My experiments screening siRNA sequences for NF-κB proteins show that it is possible to knock down total NF-κB activity with MnNP delivered siRNA. Although siRNA sequences for IKKβ, p65, and p52 all resulted in significant knockdown, it is important to establish whether or not these proteins will be efficacious targets. Although p65 is implicated in producing smoldering inflammation in the tumor microenvironment, it is also responsible for survival signaling in macrophages. p65 is not an optimum target because knocking down p65 could potentially induce apoptosis in the macrophages being targeted for phenotypic modification.[68, 72]

Viable targets for therapeutic siRNA knockdown ideally should also express increased amounts of the target mRNA while in the pathological state. qRT-PCR of TNF-α stimulated BMDMs indicates that while levels of p52 mRNA are increased upon exposure to TNF-α, levels of IKKβ do not significantly increase (Figure 3.1). There are multiple potential explanations for why increased levels of IKKβ mRNA were not detected. It is known that the classical NF-κB pathway is rapidly activated within minutes of stimulation, while alternative activation is more gradual.[66, 73, 74] If there is an increase in IKKβ mRNA, it is possible that the increase is rapidly induced, then rapidly degraded. Another alternative is that there is already enough IKKβ protein active in the cell to activate enough p50:p56 homodimers and induce a classical NF-κB response; increased production of IKKβ may not be necessary. Regardless of the reason, this lack of increase in IKKβ mRNA makes it a poor target for siRNA mediated knockdown. In addition, there are significant non-NF-κB functions of IKKβ, and knocking down this protein could potentially have off-target effects.[3]

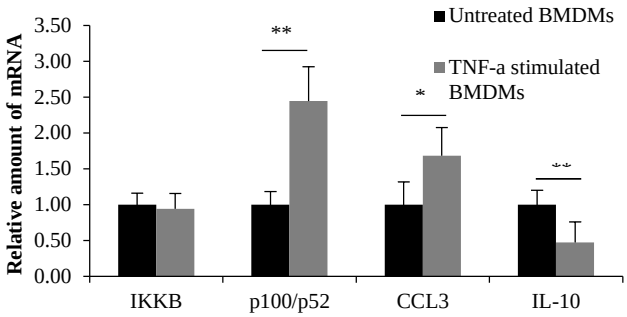

Figure 3.1: qRT-PCR of TNF-α stimulated BMDMs and unstimulated BMDMs. Activation is confirmed by significant increase in CCL3 mRNA and significant decrease in IL-10 mRNA. Levels of p100/p52 mRNA significantly increase following 6 hours of TNF-α stimulation, but the amount of IKKβ mRNA does not significantly increase. * : $P < 0.05$, ** : $P < 0.005$.

p52 is a viable target for knocking down alternative NF-κB activity in TAMs. Neither IKKβ nor p65 are attractive targets for siRNA mediated knockdown aimed at reducing the smoldering inflammation produced by TAMs. However, decreasing the smoldering inflammation from these cells is not the only therapeutic option. If the full inflammatory potential of the TAMs could be reactivated, these cells could promote a potent immune response at the site of the tumor by releasing inflammatory cytokine and inducing apoptosis and by recruiting cytotoxic immune cells of innate and adaptive immune system. This effect could be achieved by strongly activating the classical NF-κB pathway in TAMs.

Although delivering siRNA with MnNP was initially designed to knockdown NF-κB activity, it should theoretically be able to activate the classical pathway as well. Activation of transcriptional pathways by siRNA has been reported before, but only as an undesirable, off-target side effect. Because the IκBα protein inhibits activation of the classical pathway, knocking down this protein could potentially increase classical NF-κB activation. Activation of a key transcriptional pathway would be a novel approach to manipulating cell phenotype for immunoengineering. To test this hypothesis, NGL BMDMs were transfected with MnNP delivered siRNA against IκBα for 24 hours, and total NF-κB activation was measured at multiple time points during transfection. Figure 3.2 shows that while free siRNA did not induce

activation of NF-κB, and empty particles had a very minor immunogenic effect, delivery of IκBα siRNA by MnNP induced significant activation of NF-κB without any other source of stimulation.

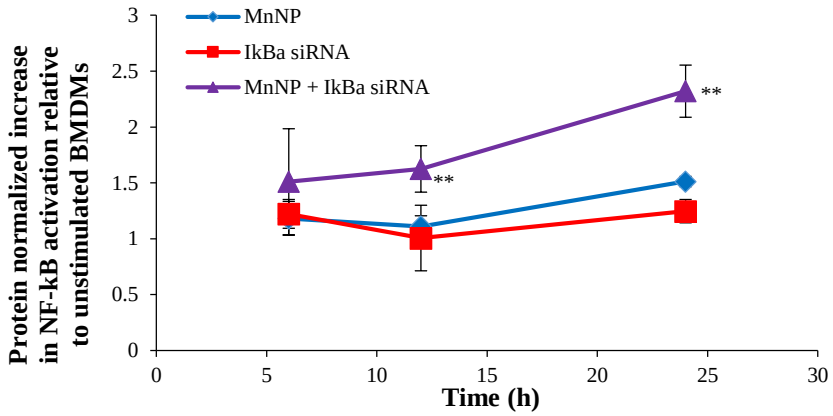

Figure 3.2: Activation of NF-κB in NGL BMDMs by MnNP delivery of IκBα siRNA without any other form of stimulation or activation. NF-κB activity is significantly increased as early as 12 hours following transfection with IκBα by MnNP, and activity has more than doubled 24 hours after transfection (** : $P \leq 0.001$). There is some small activation caused by delivery of unloaded MnNP polymer after 24 hours, but this activation is significantly less than that mediated by delivery of both MnNP and IκBα ($P = 0.005$).

This result shows a novel approach to therapeutic RNAi: using knockdown to increase activation rather than decrease activation of a transcriptionally active pathway. Knocking down the inhibitor of the classical NF-κB pathway increases total NF-κB activity, but it is important to understand if this knockdown is physiologically and therapeutically relevant. In order to understand what affect IκBα knockdown in macrophages might have on tumor cells, an IκBα knockout macrophage line was co-cultured with fluorescently labeled tumor cells (PYL) for 3 days and the co-culture was imaged at <1 and 3 days (Images courtesy of Oleg Tikhomirov). Figure 3.3 shows the IκBα knockout (IκBα k/o) macrophage/PYL tumor cell co-culture compared to a wild type macrophage line, also at 3 days co-culture with PYL cells. After 3 days, the wild type macrophages exist in stable co-culture with the tumor cells and there are no overt, morphological signs of cytotoxicity in ether cell type. However, even earlier than 1 day post co-culture, there are signs that the IκBα k/o macrophages are mediating some form of tumor cell cytotoxicity. The IκBα k/o macrophages appear to form adhesion complexes with the tumor cells and pull on the membrane of the cells. Adhesion complexes are known to play an important part in mechanisms of classically activated

macrophage cytotoxicity. Furthermore, the k/o macrophages appear to destroy the cytoplasmic compartment of the tumor cells, and by 3 days, only fragments of the tumor cells are left; The IκBα k/o macrophages have mediated some form of extracellular lysis of the tumor cells.[75, 76]

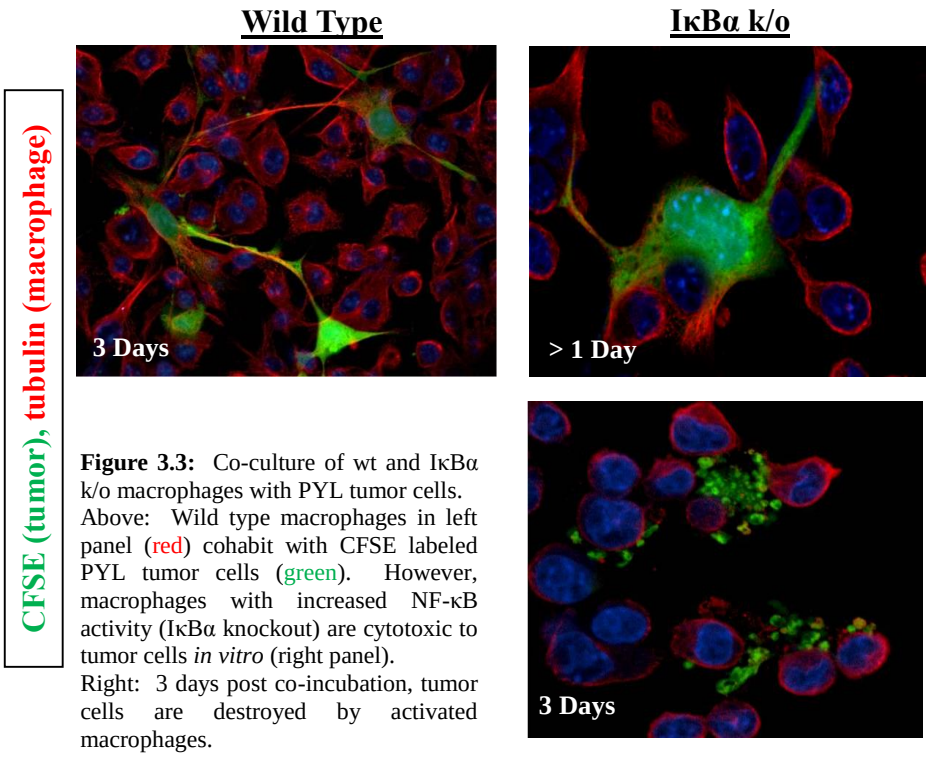

Figure 3.3: Co-culture of wt and IκBα k/o macrophages with PYL tumor cells. Above: Wild type macrophages in left panel (red) cohabit with CFSE labeled PYL tumor cells (green). However, macrophages with increased NF-κB activity (IκBα knockout) are cytotoxic to tumor cells *in vitro* (right panel). Right: 3 days post co-incubation, tumor cells are destroyed by activated macrophages.

qRT-PCR of BMDM transfected with NF-κB specific siRNA sequences by MnNP. After it was determined that it was possible to activate NF-κB by knocking down the inhibitor of the classical pathway and that IκBα k/o macrophages can be cytotoxic to tumor cells, the mRNA from BMDMs transfected with IκBα siRNA by MnNP was analyzed for potential anti-tumor indications. Figure 3.4A shows that levels of mRNA for IκBα are significantly decreased following transfection with IκBα siRNA, indicating successful knockdown at the mRNA level of IκBα. This can be contrasted to IKKβ as a classical pathway target, which I predict would not be an optimal target for mRNA level knockdown.

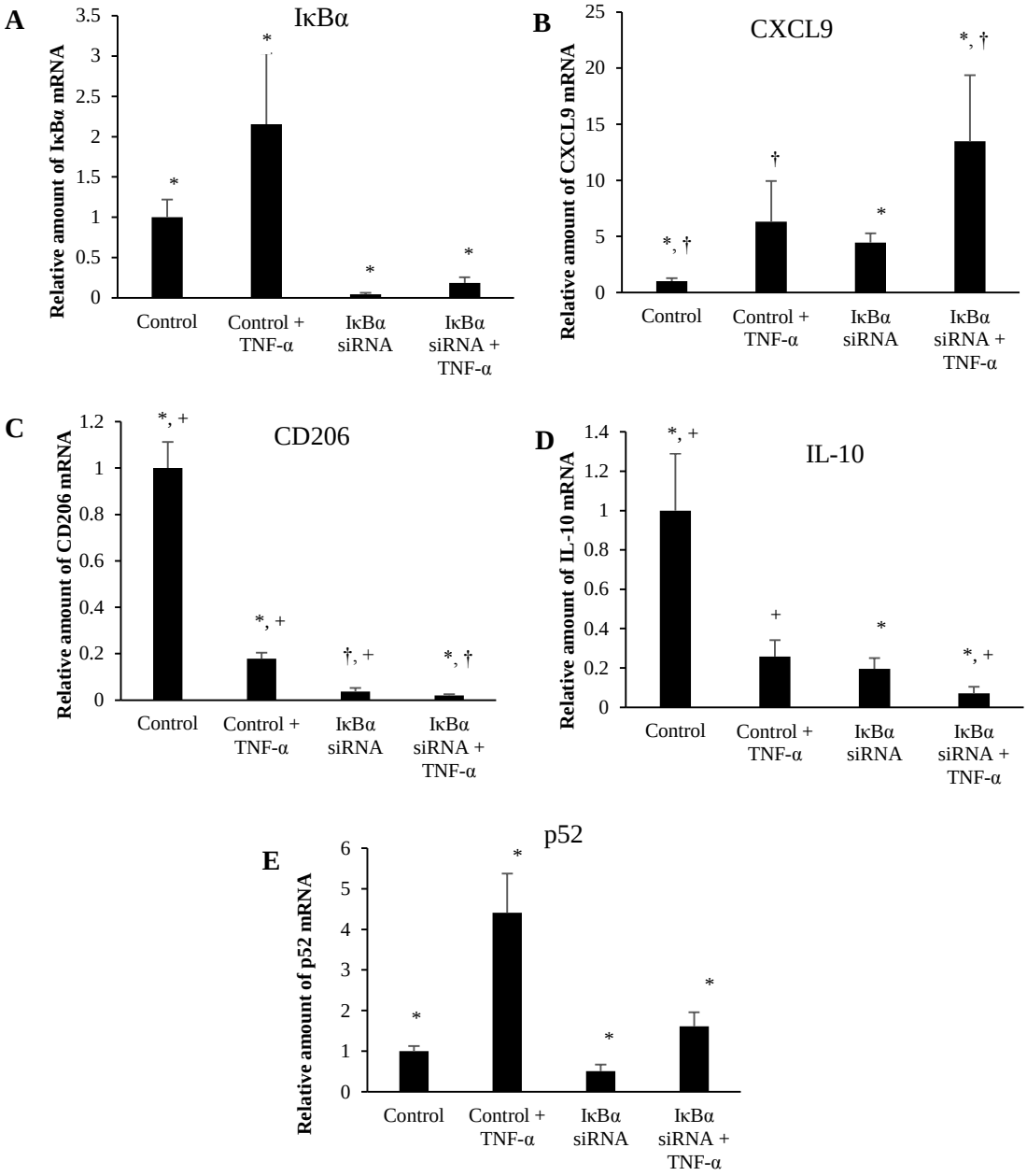

Figure 3.4: qRT-PCR of IκBα siRNA transfected BMDMs. In all cases, ANOVA indicates the presence of significant differences in the datasets ($P<0.001$) (A) IκBα siRNA significantly knocks down IκBα mRNA. Although stimulation with TNF-α increase IκBα mRNA, this effect is significantly reduced by IκBα siRNA. (B) IκBα siRNA increases mRNA for T-cell recruitment cytokine, CXCL9. The increase in CXCL9 mRNA by transfection alone is not significantly different than the increase caused by TNF-α alone. (C) IκBα siRNA decreases mRNA for the mannose receptor, CD206, an M2 and TAM phenotype marker. The combination of TNF-α and IκBa siRNA results in significantly greater decrease in CD206 mRNA. (D) IκBα siRNA decreases mRNA for IL-10, an immunosuppressive cytokine. The decrease in IL-10 mRNA by transfection alone is not significantly different than the decrease caused by TNF-α alone, but the combination of the two results in less IL-10 mRNA than either condition by itself. (E) IκBα siRNA decreases mRNA for p52. TNF-α stimulation of macrophages increases levels of p52 mRNA: p52 is a viable target for mRNA level knockdown. Transfection with IκBα siRNA reduces the increase in p52 mRNA caused by TNF-α, indicating potentially beneficial cross-talk between the two pathways which could be leveraged to act synergistically toward altering the TAM phenotype to an anti-tumor phenotype. † : $P \leq 0.01$, *, + : $P \leq 0.005$

Figure 3.4 also shows modifications in the mRNA levels of cancer-context relevant cytokines produced by macrophages. IκBα siRNA increase the amount of CXCL9 mRNA in macrophages to a level that is not significantly different from levels of CXCL9 mRNA in TNF-α stimulated macrophages. CXCL9 is a chemotactic signal that recruits $CD8^+$ T-cells and NK cells.[77] Furthermore, the combination of IκBα siRNA and TNF-α acts in an additive fashion, resulting in significantly more CXCL9 mRNA than either of the two treatments alone. Increasing CXCL9 in the tumor microenvironment has been shown to enhance antitumor immunity in murine breast cancer models.[78] It has also been reported that intermediate CXCL9 signaling is necessary for T-cells to respond to other recruitment signals, such as IL-12.[79] This indicates that knockdown of IκBα in TAMs could recruit activated, cytotoxic cells of the innate and adaptive immune systems to the tumor microenvironment. The recruitment of T-cells to solid tumors has been the major focus of many efforts to induce tumor immunity in several types of cancer.[54, 55, 80] Recruitment of T-cells by modified macrophages in the tumor is another potential method of activating adaptive tumor immunity.

MnNP-delivered IκBα siRNA also decrease levels of phenotypic markers indicating a pro-tumor, immunosuppressive macrophage phenotype. Increased levels of the mannose receptor, CD206, in macrophages indicates an alternatively activated phenotype and/or a TAM phenotype.[12, 29] Both TNF-α and IκBα siRNA decrease mRNA for CD206 in macrophages. The combination of the two also significantly decreases CD206 mRNA. This effect is particularly important because the mannose receptor is the target of the mannose ligand on the MnNP surface. Transfecting macrophages with IκBα siRNA effectively decreases the amount of target on the macrophages surface. This effect could ensure that only macrophages with a strong TAM phenotype, cells with more CD206 on their surface, have enhanced, endosomal uptake of the particles. Ideally, the MnNP would preferentially transfect macrophages with high levels of CD206. Transfection would then alter the phenotype of the macrophage toward classical immune activity, reducing the amount of CD206 on the cell surface, preventing further, unnecessary transfection. The MnNP would then be free to transfect other resident macrophages with high levels of CD206 or other recruited macrophages with a TAM phenotype. The MnNP could also potentially act as a surveillance mechanism if

there are particles retained extracellularly in the tumor, re-transfecting macrophages if they begin to re-adopt a TAM phenotype and express CD206 at their surface.

IκBα siRNA also decreases IL-10 mRNA in macrophages. IκBα siRNA decreases the amount of IL-10 mRNA in macrophages to a level that is not significantly different from levels of IL-10 mRNA in TNF-α stimulated macrophages and the combination of IκBα siRNA and TNF-α results in significantly less IL-10 mRNA than either of the two treatments alone. IL-10 is a potent immunosuppressive cytokine and is implicated in creating the TAM phenotype by paracrine signaling from tumor cells and other TAMs, and by autocrine signaling as well.[58, 81] IL-10 has been reported to specifically inhibit the classical NF-κB pathway by increasing the amount of cytoplasmic p105 and p50:p50 homodimers, and by reducing p65 translocation into the nucleus.[82, 83] Treatment of macrophages with IL-10 reduces classical NF-κB responsiveness to stimulating cytokines like LPS and TNF-α by reducing nuclear translocation of p65:p50 homodimers, which are responsible for much of the classic inflammatory response governed by NF-κB, and by increasing translocation of p50:p50 homodimers which strongly inhibit the classical immune response.[84] In many cases p50 homodimers inhibit transcription of NF-κB gene targets. However, p50 homodimers are reported to activate production of IL-10 in macrophages.[53, 85] Furthermore, IL-10 stimulation of macrophages does not affect the ability of the alternative NF-κB pathway in these cells to respond to TNF-α and other TNF protein family members, many of which are present in the tumor microenvironment.[83]

These studies indicate that IL-10 creates a powerful feedback loop in TAMs. IL-10 stimulation reduces classical NF-κB responsiveness to TNF-α, but does not completely eliminate the effect. This would result in much lower levels of inflammatory cytokine production in response to the constant presence of inflammatory cytokines in the tumor microenvironment, producing smoldering inflammation. In addition, the alternative pathway is free to respond to a smaller subset of these cytokines, activating the tumor-supportive effect of this pathway. Finally, IL-10 stimulation activates a positive feedback loop of IL-10 production, effectively locking the macrophages in the TAM phenotype, unless something can disrupt this

signaling loop. Transfection with IκBα siRNA not only decreases IL-10 mRNA, but it also increases the transfected macrophages' ability to respond to TNF-α, indicating that it might be an effective therapeutic agent for disrupting the IL-10 positive feedback loop and abrogating the TAM phenotype.

Finally, the results suggest that there is a certain amount of cross-talk between the two pathways that could be leveraged to reduce the negative effects of the TAM phenotype. This result is corroborated by the fact that mRNA levels of p52, which increase following TNF-α stimulation, are decreased by transfection with IκBα siRNA. This effect may be the result of direct or indirect crosstalk, and could indicate the potential possibility of decreasing the pro-tumor effects of the alternative NF-κB pathway by knocking down the IκBα and activating the classical pathway.

To confirm that the effects of MnNP delivered siRNA shown in Figure 3.4 were not artifacts caused by macrophage interaction with the MnNP transfection agent, MnNP were used to transfect BMDMs with a scrambled siRNA sequence following the same protocol. Figure 3.5 shows that there are no significant differences between macrophages transfected with scrambled siRNA sequences and untransfected macrophages for mRNA for IκBα, p52, CXCL9, and IL-10. There is some significant increase in CD206 upon uptake of the MnNP. This is consistent with the reported mechanism of CD206 production following CD206 binding events. It has been reported that as the number of CD206 binding and endosomal uptake events increases, so does production of CD206.[86] This increase in receptor production following activation helps to explain the rapid recycling of this receptor.[87] The small increase in CD206 following MnNP delivery highlights the ability of IκBα knockdown to reduce CD206 mRNA: MnNP-delivered, IκBα siRNA alone reduces CD206 mRNA by approximately 95%.

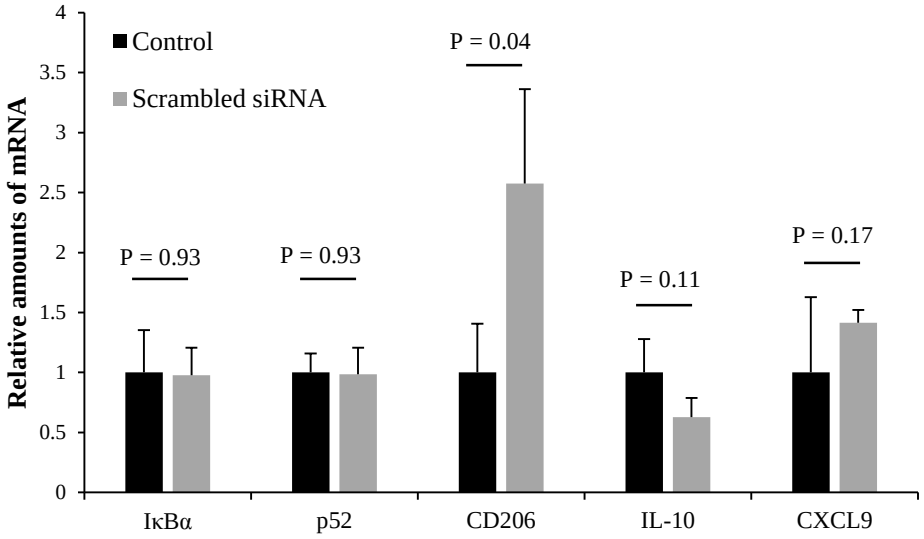

Figure 3.5: qRT-PCR of scrambled siRNA transfected BMDMs. There is no significant decrease in mRNA levels between the two groups for IκBα, p52, IL-10 and CXCL9. There is a significant increase in CD206 mRNA following culture with MnNP loaded with a scrambled siRNA sequence. This is consistent with previous reports that activation and endosomal transport of the mannose receptor increases mannose receptor production in macrophages.

Conclusions

To facilitate delivery NF-κB specific siRNA to tumor associated macrophages, we have developed a targeted polymer nanoparticle that encapsulates and protects siRNA sequences. The nanoparticles have a mannosylated surface designed to target the mannose receptor, which is upregulated in TAMs and M2 macrophages. MnNP can deliver efficacious amounts of siRNA for manipulating the NF-κB pathways in macrophages and are more specific than commercial transfection agents. The targeting moiety on the surface of the particle also enhances transfection efficacy and speed compared to untargeted nanoparticles with the same core structure and siRNA loading. I have utilized MnNP-delivered siRNA to accomplish the goal of activating classical NF-κB activity by knocking down the inhibitor of the classical pathway, IκBα. There have been reports of siRNA activating transcriptional pathways in cells, but this has always been seen as an undesirable, off-target effect of transfection in general. Deliberate activation of a specific transcriptional pathway by using siRNA to knockdown an inhibitor of the pathway has not been reported

and is a novel mechanism for manipulating cell phenotype. Following delivery of IκBα siRNA to macrophages by MnNP, mRNA for IκBα was decreased and mRNA for a T-cell recruitment cytokine CXCL9 was increased. Furthermore, mRNA for the mannose receptor and for IL-10 were decreased, indicating a loss of immunosuppressive function and a potential mechanism for disrupting the positive feed-back loop between TAMs and tumor cells, which is implicated in sustaining the TAM phenotype. In the future we hope to utilize this strategy to modulate NF-κB in TAMs *in vivo*, and activate tumor immunity in solid tumors.

CHAPTER 4

Biocompatible mannosylated endosomal-escape nanoparticles enhance selective delivery of short nucleotide sequences to tumor associated macrophages *in vivo*

Introduction

The tumor supportive stroma has been identified as an attractive target for therapeutic intervention in solid tumors. While most tumors exhibit a large degree of cellular heterogeneity, the tumor stroma is potentially more homogenous with respect to local stromal cell phenotype.[88] Tumor associated macrophages (TAMs) are directly involved in establishing a pro-tumorigenic local microenvironment in many tumor types and TAM presence is predictive of poor prognosis and survival in mouse models of human breast cancer and in multiple human cancers.[15, 89] Data show that TAMs are a viable therapeutic target in cancer treatment and that ablating these cells can have a powerful anti-tumor effect. Rather than ablate these important modulators of immunity, another proposed solution is to target pro-tumor macrophages with a therapeutic agent that can alter their behavior to induce an acute, but strong immunogenic phenotype capable of stimulating anti-tumor immunity.[90, 91]

Systemic delivery of therapeutic nanoparticles is limited by the many mechanisms by which these particles are rapidly cleared from circulation. In almost all cases of systemic delivery, most of the nanoparticle dose is cleared by the reticuloendothelial system or by the kidneys. Particles can also be non-specifically taken up by the spleen. Only a small percentage of the dose makes it to the target site, but even a small percentage of the total dose can have a therapeutic effect. Systemic delivery of nanomaterials for cancer therapy often relies on passive delivery and retention in tumors, caused by the enhanced permeability and retention effect.[92] Delivery to the target cell population is often enhanced by adding a targeting moiety to the surface, as is the case with the mannosylated nanoparticles used for these studies. Another method used to enhance delivery and retention in tumors is to spatially confine the nanoparticle dose in or near the

tumor.[93] For the *in vivo* experiments reported here, all nanoparticle doses were delivered to a spatially confined compartment using clinically relevant delivery methods (either direct intratumoral injection or direct injection into the peritoneum or lung) in order to mitigate the drawbacks associated with systemic injection.

In this study, I build upon previously published work to demonstrate that these MnNP are biocompatible *in vitro* and *in vivo* at physiologically relevant doses, provide evidence for the efficacy of the CD206-targeting mannose ligand on the surface of the particles, and demonstrate the effective delivery of protected nucleotides to TAMs.

Materials and Methods

Fabrication of nucleotide loaded MnNP. Nucleotide loaded MnNP were fabricated as described in Chapter 2.

Particle zeta potential measurements. Average nanoparticle zeta potential (ζ) was determined by laser Doppler electrophoresis (LDE) using a Malvern Zetasizer Nano ZS (Malvern Inst. Ltd., Malvern, UK). Briefly, siRNA oligomer solution (50 μM, deionized water) was mixed with two times the volume of mannosylated nanoparticle solution (4 mg/mL, PBS) and reacted at room temperature to allow complexation. Aliquots were removed and diluted approximately 200-fold in molecular biology grade water for zeta potential measurement at time points relative to initiation of the nanoparticle-siRNA complexation reaction. Zetasizer measurements were performed at 25 °C with a scattering angle of 175°.

Cell culture. Unless otherwise stated, all primary cells isolated for use in this study were maintained in DMEM (Corning, MT-10-13-CV) with the addition of 10% (vol:vol) FBS and 1% Pen Strep (Gibco) at 37°C in a 5% CO_2 humidified atmosphere.

***In vitro* biocompatibility measurements.** Bone marrow derived macrophages (BMDMs) were made by harvesting bone marrow from wild type mice on an FVB background. The media for these cells was supplemented with media from L-129 fibroblasts as a source of M-CSF.[42] The bone marrow was

cultured for 6 days in the M-CSF supplemented media and the resultant BMDMs were scraped from their plates and re-plated as necessary for further experiments. For *in vitro* viability experiments, BMDMs were plated in 12-well plates at a density of 300,000 cells per well (approximately 80,000 cells/cm^2). BMDMs were transfected for 24 hours at 37°C with MnNP-siRNA complexes with a scrambled siRNA sequence at 10 nM and 50 nM concentrations of siRNA with accompanying MnNP concentrations as described above, with and without 6 hours of TNF-α stimulation (10 ng/ml) following transfection. A second set of BMDMs were transfected with the same siRNA using Lipofectamine 2000 (10:1, vol:vol, Lipofectamine:siRNA) (Ambion) for 24 hours with and without TNF-α stimulation. 2 minutes of incubation with Triton x-100 was used as a negative control for cell membrane viability. To stain cell membranes for an exclusion viability assay, samples were incubated with Trypan Blue for 5 minutes, and the number of viable and non-viable cells were counted (over 1000 cells per sample, N=3 for each condition).

***In vivo* biocompatibility measurements.** All animal experiments were approved by the Vanderbilt University Institutional Animal Care and Use Committee. Wild type FVB mice were i.v. injected via the retro-orbital route with MnNP-scrambled siRNA complexes (siRNA: scrambled negative control sequence, Ambion) at 5 mg/kg of particles every 24 hours for 3 doses. 24 hours after the final injection, blood serum was taken from the mice and analyzed at the Vanderbilt Translational Pathology Core Laboratory. Alanine transaminase (ALT) and aspartate transaminase (AST) levels were measured as an indicator of hepatic function and blood urea nitrogen (BUN) and serum creatinine (CREAT) as an indicator of renal function.

***In vivo* delivery of fluorescently labeled DNA to murine mammary PyMT TAMs.** Palpable tumors from 12-week old PyMT mice were used to examine the nucleotide delivery efficacy of MnNP *in vivo*. A 21 base pair, Cy3-labled DNA sequence was purchased from Sigma for complexation with MnNP. Three ellipsoidal tumors were selected from each mouse from three separate glands with an average tumor volume of 5.2 ± 1.9 cm^3. Tumors were selected based on their isolation from any other large tumor and on uniformity of size and shape. One tumor from each mouse received an injection of MnNP-DNA_Cy3 complexes into the centroid of the tumor at a dose of 5 mg/kg, one tumor received an equivalent dose of

cy3-labeled DNA, and one tumor received a 100 ul PBS injection. The tumors were injected in this fashion every 24 hours for three total doses. 24 hours after the final dose, the tumors were removed, homogenized, and the TAMs were isolated with a 45 minute rapid adhesion protocol. Cy3 fluorescence was measured in each sample with a Tecan Infinite M1000-Pro plate reader as an indicator of DNA delivery with 12 measurements per well in a filled circular pattern. The data are shown after background subtracting fluorescent averages from the tumors receiving MnNP-DNA_Cy3 complexes normalized to the tumor samples receiving free DNA_Cy3.

***In vivo* delivery of fluorescently labeled DNA to murine solid ovarian tumor TAMs.** ID8 cells were generously gifted by Drs. D. Khabele and A. Wilson of the Vanderbilt Ingram Cancer Center. Cy5-labled DNA was purchased from Sigma (21 base pairs). ID8 cells were injected into the peritoneal cavity of mature C57B16 female mice (10 million cells per mouse). 60 days after ID8 cell injection, the mice began to present with increased total mass and distended abdomens, indicating the beginning stages of ascites development. The mice received 2 injections, 24 hours apart of untargeted particles with DNA_cy5 (5 mg/kg, 3 mice) or mannose receptor targeted particles with DNA_cy5 (5 mg/kg, 3 mice). 24 hours after the last injection, the mice were euthanized and the tumors on the peritoneum were removed and homogenized. The TAMs were isolated with a 45 minute rapid adhesion protocol. Cy5 fluorescence was measured in each sample with a Tecan Infinite M1000-Pro plate reader as an indicator of DNA delivery with 12 measurements per well in a filled circular pattern.

Murine lung metastasis tumor model and delivery of nanoparticles via intubation. 0.5 million L129 PyMT tumor cells were injected via tail vein into wildtype FVB mice.[43] 2 weeks after injection, each mouse was anesthetized with isoflurane and placed on a tilted rodent work stand in the supine position and restrained in position by an incisor loop. The tongue was extruded using forceps, the mouse intubated, and given a 5 mg/kg dose of either MnNP-DNA_Cy5 complexes (n=5) or OHNP-DNA_Cy5 complexes (n=3). Control animals received a 60 ul dose of sterile PBS. After the tubing was removed, the mice were observed until normal respiration resumed.

IVIS imaging of whole lungs. Whole lungs were removed 6 hrs post-injection from mice receiving MnNP-DNA_Cy5 via intubation (n=2) or via i.v. injection (n=2), and an untreated control mouse. All lungs were tumor bearing. Lungs were perfused and inflated with cold PBS and then imaged for Cy5 fluorescence using a Xenogen IVIS 200 bioluminescent and fluorescent imaging system and Living Image software at the Vanderbilt University Institute of Imaging Science.

Isolation of lung cells and flow cytometry. Lungs were perfused with sterile PBS and digested as described above. Single cell suspensions were kept at 4°C and incubated with 1% BSA in PBS to reduce non-specific antibody binding. The panel of antibodies used in these experiments included CD45-PE-Cy7 (clone 10-F11), Gr1-Alexa Fluor 700 (clone RB6-8C5), and CD11B-APC (clone M1/70) (all from BD Bioscience). Flow cytometry was performed using a BD LSR II flow cytometer (BD Bioscience) and data were analyzed with FlowJo software (TreeStar). To identify the myeloid cell subset in the lung homogenate, I began by sorting cells based on CD45 expression. To further differentiate cell populations, I sorted cells based on the presence of CD11b and the presence or absence of Gr1. I defined the macrophage population as being $CD45^+/CDllb^+/Gr1^-$ and both monocytes and polymorphonuclear (PMN) cells as being $CD45^+/CDllb^+/Gr1^+$.[94] These simple flow panels allowed us to isolate normal macrophages and TAMs from other myeloid cell populations that could potentially uptake delivered nanoparticles through non-specific mechanisms.[95, 96]

Results and Discussion

Particle-siRNA complexation and biocompatibility. MnNPs were synthesized as previously reported.[13] The chemical structure of the particles is shown in Figure 4.1A.

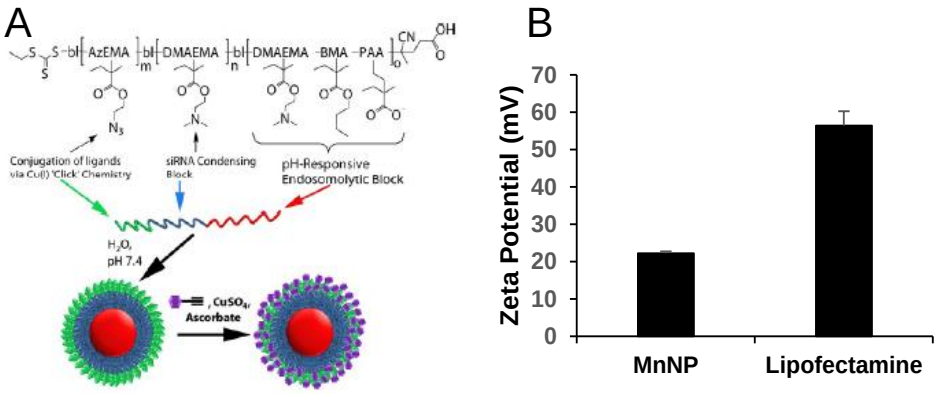

Figure 4.1: (A) Schematic representation of the mannosylated endosomal escape nanoparticle illustrating the pH-responsive core (red), the siRNA condensing block (blue), the modular 'clickable' surface (green), and the mannose surface functionalization (purple). (B) Zeta potential measurements of MnNP show a significantly milder surface charge as compared to commercial transfection agent, Lipofectamine 2000. (P = 0.003, N=3)

Commercial transfection agents, such as Lipofectamine, possess strong, positive surface charges which facilitate their ability to deliver siRNA and other nucleotides into cells. This same surface charge renders commercial transfection agents unacceptable for *in vivo* use; they exhibit low biocompatibility due to aggregate formation and cytotoxicity. Strongly cationic structures have the potential to adsorb anionic serum proteins and lose function through aggregation or become opsonized and rapidly cleared from the blood compartment. Therefore, net surface charge of the formulated delivery system is known to be an important determinate of *in vivo* function. The cationic charges in MnNPs are designed to be largely shielded from surface presentation to optimize their potential for *in vivo* use. The success of this shielding strategy was confirmed by the moderately positive zeta potential of approximately +20 mV as measured by dynamic light scattering (Figure 4.1B) in comparison with Lipofectamine 2000, a commonly used commercial transfection agent with a zeta potential of more than +50 mV. Charge-based considerations are of paramount importance in the context of intravascular administration; however, similar considerations are operative for the intraperitoneal and tracheal delivery used in these studies. Thus, the low cationicity of MnNPs may optimize successful siRNA delivery to TAMs by the routes of administration considered here.

Cationic charge mediates strong interactions with anionic cell membranes to facilitate delivery of cargo *in vitro*, but also may destabilize cells and be responsible for dose-limiting toxicity. I determined the effect of MnNP on membrane viability in bone marrow derived macrophages (BMDMs) as an *in vitro* measurement of the biocompatibility of the MnNP-siRNA complexes (Figure 4.2). siRNA was delivered at low (10 nM) and high (50 nM) concentrations in the presence or absence of a second immunostimulatory cytokine, TNF-α (10 ng/ml), a common tumor promoter in the tumor microenvironment.[97, 98] After 24 hours of incubation with MnNP-siRNA there was no significant decrease in BMDM membrane integrity in samples transfected with MnNP as measured by Trypan Blue staining.[99] The high siRNA concentration had a slight effect on BMDM membrane viability in the context of the addition of TNF-α, but this effect was not significant. In contrast, in the presence of TNF-α, transfection with the commercial agent, Lipofectamine 2000, resulted in a significant decrease in viability (21-23%). Lipofectamine is a mixture of positively charged lipids; the strongly positive surface charge on the lipid transfection complex results in an efficacious *in vitro* transfection agent, but significantly decreased biocompatibility *in vivo* due to strong interactions with the plasma membrane of non-targeted cells.[100] In contrast, MnNP-siRNA complexes possess only a mildly positive surface charge, resulting in increased biocompatibility and suitability for both *in vitro* and *in vivo* transfection.

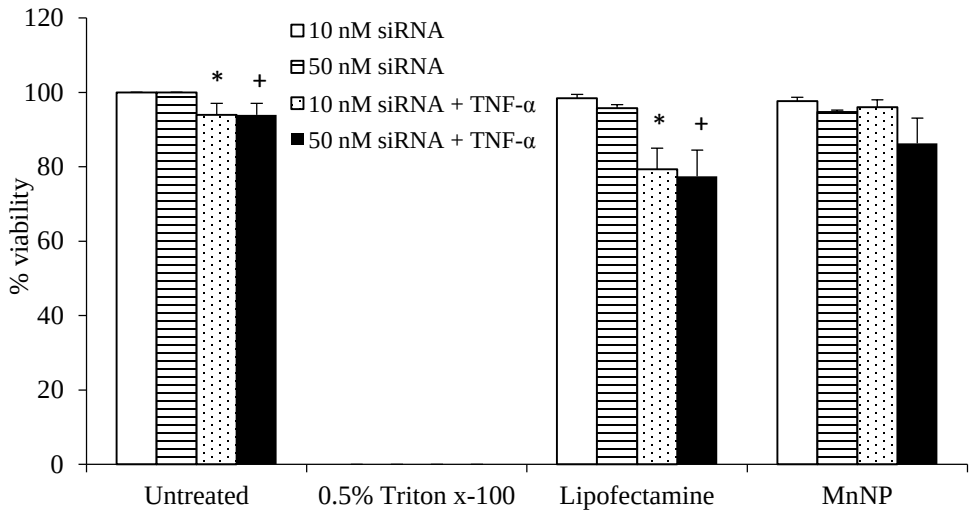

Figure 4.2: Transfection of BMDMs in vitro with MnNP-siRNA complexes results in no significant loss in membrane viability, even with secondary stimulation from 10 ng/ml TNF-α stimulation for 6 hours. There is significant loss in viability associated with the use of Lipofectamine as a transfection agent under these conditions. (*, +: $P < 0.05$, N=3 for each condition)

To test *in vivo* biocompatibility, wild type FVB mice were intravenously (i.v.) injected with MnNP-scrambled siRNA complexes at 5 mg/kg once daily for 3 consecutive days. 24 hours after the final injection, blood serum was analyzed for alanine transaminase (ALT) and aspartate transaminase (AST) levels as an indicator of hepatic function and blood urea nitrogen (BUN) and serum creatinine (CREAT) as an indicator of renal function. No significant change in liver or kidney function was observed following 3 sequential doses every 24 hours with MnNP, consistent with a lack of acute, organ level toxicity (Table 4.1). Average serum creatinine was slightly lower than the normal range, but the difference is not large enough to indicate renal damage.[101] Since I anticipate that MnNPs will clear the cardiovasculature primarily through liver/spleen/reticuloendothelial mechanisms and that molecular components from disassembled micelles (if any) will be sufficiently small for renal excretion, the lack of significant dysregulation in liver and kidney characteristics suggests both nontoxicity and serum stability.

Table 4.1: Analysis of blood serum enzyme levels revealed no significant changes in liver or kidney function in mice receiving three, 5 mg/kg i.v. doses of MnNP-siRNA complexes, 24 hours apart.

	Mouse Number						
	1	2	3	4	Average	σ	normal range
ALT (U/L)	37	49	73	105	66	30	26-120
AST (U/L)	96	86	213	140	133.75	57.80	69-191
BUN (mg/dL)	21	23	27	23	23.5	2.51	19-34
CREAT (mg/dL)	0.4	0.3	0.3	0.4	0.35	0.05	0.4-0.6

MnNPs deliver fluorescently labeled nucleotides to murine TAMs *in vivo*. In order to test the *in vivo* efficacy of the TAM-targeted MnNP, I delivered MnNP carrying fluorescently-tagged, scrambled DNA strands to murine tumors in several tumor models. PyMT mice have spontaneously developed palpable mammary tumors with dimensions ≥ 1 cm at 12 weeks and the tumors have a necrotic core with significant immune cell infiltration and TAM population.[52, 102] Due to the poorly vascularized nature of this tissue, cells and fluid entering the tumor are retained in the local microenvironment longer than they would be retained in normal tissue.[92, 103] I directly injected MnNP-DNA conjugates into the center of the tumor for a well contained depot of particles that would co-localize with TAMs (Figure 4.3A). I observed no adverse effects of multiple, direct MnNP injections.

Formulation with MnNPs significantly increased DNA_Cy3 delivery to TAMs in murine breast tumors (Figure 4.3B). Intratumoral injection of a fluorescently labeled DNA mimic of siRNA resulted in nearly 2-fold greater TAM uptake compared to unformulated control DNA_Cy3 administered to another mammary tumor in the same mouse. These data suggest that the MnNP formulation is interacts with TAMs in a persistent way, noting that this study was carried out as three injections, each separated by 24 hours. This demonstrates that injecting MnNPs directly into a primary tumor can successfully deliver nucleic acid

material to TAMs. The direct injection approach avoids the potential issues associated with intravascular administration of MnNPs.

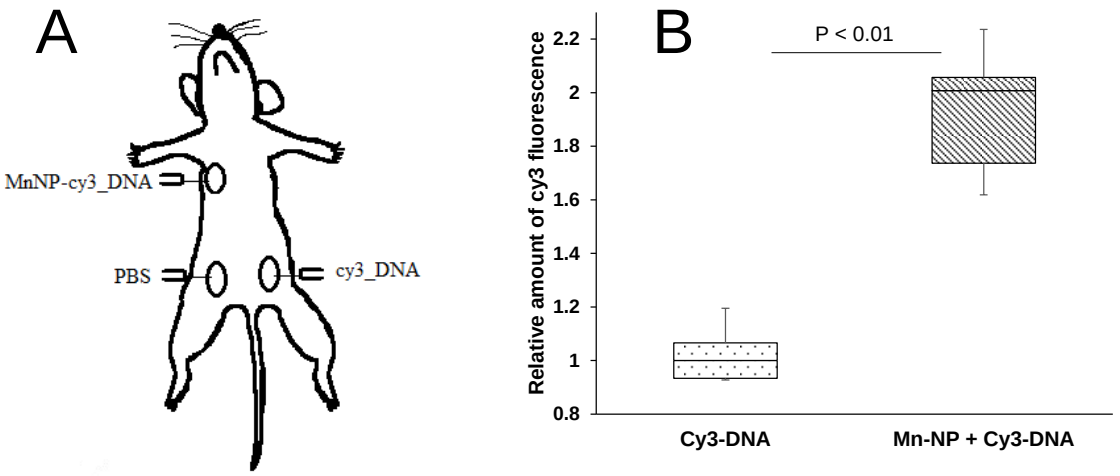

Figure 4.3: (A) Diagram of mammary tumor injection scheme for PyMT mice. Three isolated tumors from each mouse (N=3) were selected based on uniformity of size and shape. The tumors were injected 3 times, 24 hours apart with MnNP-DNA_Cy3 complexes, free DNA_Cy3, or PBS into the center of each selected tumor. The TAMs were isolated from each tumor and analyzed for cy3 fluorescence. (B) There was a statistically significant increase in Cy3 fluorescence in TAMs from tumors that received MnNP-DNA_Cy3 as compared to non-specific DNA_Cy3 phagocytosis.

MnNPs facilitated a similar increase in *in vivo* delivery of DNA_Cy5 to TAMs in a murine ovarian tumor model (Figure 4.4).[104] The solid tumors in this implanted ovarian tumor model contain a significant TAM population and the ascites fluid generated contains a large amount of blood and immune cell infiltrate composed largely of TAMs.[105-109] Evidence specifically supports mannose interaction of the MnNPs with TAMs in peritoneal tumors as DNA_Cy5 fluorescence is significantly elevated following MnNP delivery in comparison with identical, but non-mannosylated, hydroxyl-capped NPs. This result confirms the persistence of DNA_Cy5 delivery over two intraperitoneal injections spaced 24 hours apart. The environment of the ovarian tumors is somewhat unique in that prior to extremely late stages of progression, tumors are confined within the peritoneal compartment. This data provides evidence that an approach in which MnNPs are injected directly into the peritoneal cavity can successfully deliver nucleic acid material to TAMs without the potential complications associated with intravascular delivery.

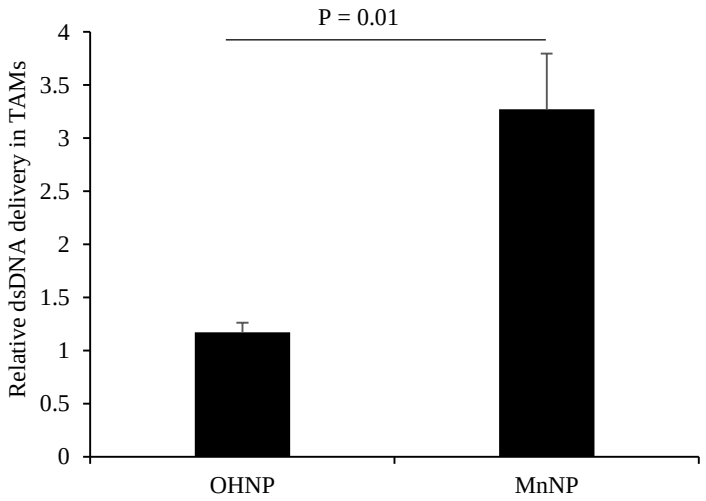

Figure 4.4: Cy5 fluorescence is significantly increased in murine ovarian tumor TAMs when Cy5-labeled DNA is delivered with mannosylated nanoparticles in vivo as compared to labeled DNA delivered with non-targeted nanoparticles. (n=3 mice)

The third *in vivo* model used to demonstrate MnNP targeting of TAMs was a model in which PyMT mammary tumor cells are injected via the tail vein to establish tumors in the lungs (Figure 4.5A). This simulates primary mammary cells that have seeded into the lungs and established metastatic growth. DNA_Cy5 carrying nanoparticles were delivered directly into the metastasis bearing lungs via intubation. This delivery method was chosen for multiple reasons: not only are the nanoparticles spatially contained within the lungs, but intubation is a clinically relevant delivery method that results in longer lung retention of the delivered therapeutic compared to systemic delivery.[110] Figure 4.5B shows that 6 hours after administration, MnNP delivered via intubation are detected in the lungs in greater amounts than MnNP delivered i.v. This image also demonstrates that delivery via intubation perfused the MnNP solution throughout the entire lung. Flow cytometry analysis performed 24 hours after particles were delivered after particles were delivered via intubation shows that approximately 40% of $CD11b^+$ myeloid cells contain DNA_Cy5 formulated with MnNPs (Figure 4.5C). This population is primarily composed of macrophages and granulocytes with some dendritic cells (DCs) and natural killer (NK) cells. DNA_Cy5 was detected in a relatively small number of non-myeloid cells, on the order of 2% in the same samples of lung homogenate.

Furthermore, DNA_Cy5 uptake by $CD45^+/CDllb^+/Gr1^-$ macrophages is significantly increased in this model through formulation with MnNP as compared with DNA_Cy5 formulated with untargeted OHNP (figure 4.5D). DNA_Cy5 uptake is not enhanced by mannose presentation on the NP corona in PMN cells and monocytes ($CD45^+/CDllb^+/Gr1^+$) (Figure 4.5D); there is no significant difference in DNA_Cy5 delivery between MnNP and OHNP formulations with these cell types. These results are consistent with strong, mannose-dependent delivery to macrophages and weak, non-specific delivery (presumably by phagocytosis) to PMN cells and monocytes. Intubation enables direct access to lung tumor TAMs for NPs, avoiding NP dilution and other challenges resulting from intravascular administration. This data demonstrates that mannose decoration mediates preferential delivery of NPs to TAMs but not non-myeloid cell types that are co-located with the TAMs in this model system.

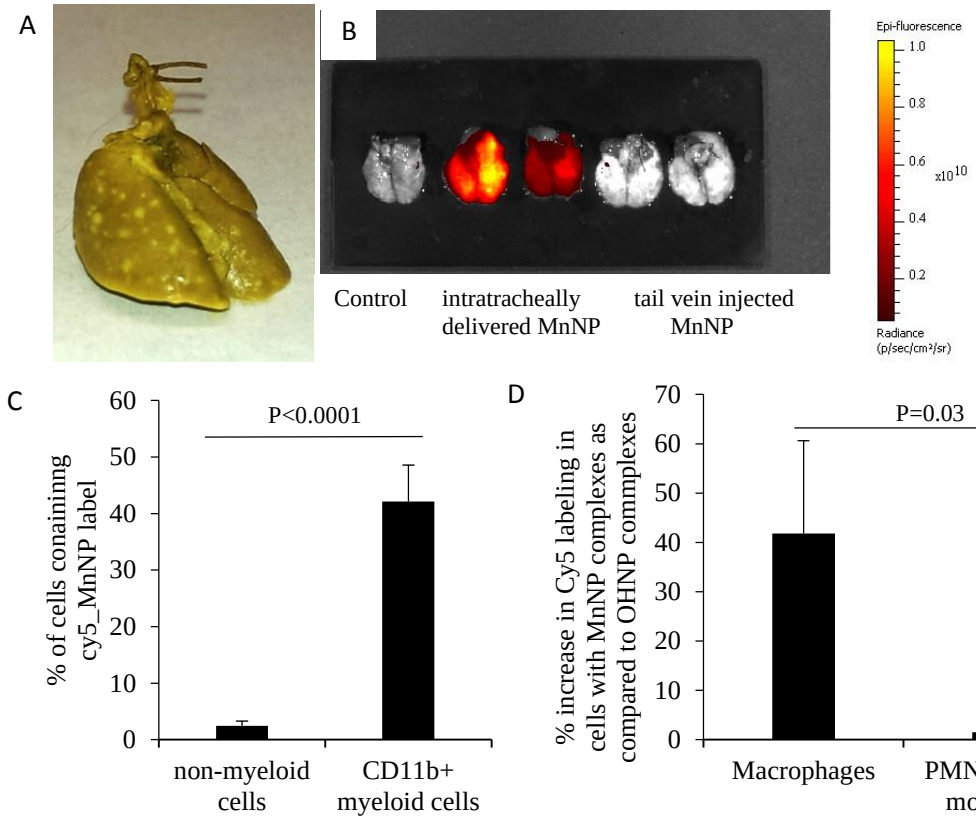

Figure 4.5: MnNP have enhanced uptake in TAMs associated with mammary lung metastases using an intubation delivery model. (A) Metastases are visualized in the lungs ex vivo following inflation with Bouin's fixative. Tumors appear white against the normal lung, which stains yellow. (B) IVIS imaging of lungs ex vivo shows intubation administration of MnNP results in more than 10 times the Cy5 fluorescence vs intravenous administration of MnNP as visualized 6 hours after delivery. (C) Flow cytometry reveals minimal uptake of MnNP (approximately 2%) in non-myeloid cells. There is significantly more uptake of MnNP in CD11b+ myeloid cells. (D) MnNP show 40% increased uptake by macrophages as compared to OHNP. There is no significant difference in nanoparticle uptake between MnNP and OHNP in PMN cells and monocytes.

The design of siRNA delivery vehicles intended for intravascular administration leading to tissue-specific accumulation is an enormous, multidimensional challenge. Such a construct must sequester and protect siRNA, avoid adverse effects resulting from interactions with serum proteins and the formed elements of the blood, possess sufficient blood compartment half-life for robust extravasation and delivery in the target tissues and offer a mechanism for preferential retention. Nonspecific toxicity must also be low. In addition, once localized, the carrier must facilitate cellular entry and endosomal escape to provide optimal conditions for effective intracellular RNAi. Despite the significant and broad potential clinical applications of RNAi, these barriers limit practical use of siRNA in humans.

Many potential clinical uses of siRNA may be approachable from other, non-intravascular, routes of administration. In this study, I assessed the capacity of an advanced nanoscale delivery system, designed for siRNA protection, preferential interaction with cells displaying CD206 and endosomal escape to facilitate efficient RNAi in models with clinicl relevance using methods that avoid intravascular administration.

This study is the first to demonstrate mannose-mediated preferential siRNA delivery to TAMs *in vivo*. *Ex vivo* studies inform three subsequent *in vivo* treatment approaches, each employing local/regional routes of administration that avoid the significant obstacles and design challenges associated with intravascular administration. Some additional advantages common to NP delivery approaches that are confined to local/regional tissues is avoidance of the liver delivery and rapid urinary clearance that are significant limiters for successful intravascular administration of siRNA delivery vehicles. Importantly, the characterizations obtained in *ex vivo* experiments with TAMs are predictive of potential *in vivo* efficacy.

I demonstrated that formulation of an siRNA surrogate into the MnNP construct enables preferential delivery to TAMs following intratumoral injection. Many characteristics likely contribute to this result, including the slightly positive zeta potential of the MnNP relative to free polynucleotide and protection against enzymatic degradation. *In vivo* stability and biocompatibility of the MnNP is also inferred from this result, consistent with previous studies and confirmed explicitly in this work by a more rigorous, intravascular study. Intratumoral administration has potential as an adjuvant therapy for primary, recurrent breast cancers, but likely is more suitable for other cancers that can be individually identified and present near the skin surface, such as head and neck cancers or melanoma.

MnNPs administered intraperitoneally effectively deliver nucleotide payloads to TAMs in the distributed tumor burden associated with ovarian cancers. This study provides the clearest evidence that mannosylation is responsible for TAM selectivity *in vivo*, in agreement with previous work and the known surface display of CD206 on macrophages, especially pro-tumor TAMs. Multiple doses of MnNPs were well tolerated. Spatial confinement of the MnNP dose in the peritoneal cavity presumably enhances the

opportunity for interaction with ovarian TAMs relative to intravascular dosing through greater proximity and longer persistence. The ability of MnNPs to preferentially localize in lung metastasis TAMs following intubation delivery implies transport of the nanomaterials from the alveolar side of the tissue into the tumors. Mannose-dependent interaction of MnNPs with TAMs is demonstrated from a different perspective in this study relative to the ovarian results in that flow cytometry confirms both strong nucleotide delivery to TAMs and lack of delivery to non-myeloid cells. All animals tolerated the intubation and delivery of MnNPS, despite a brief, acute response to the significant fluid burden administered to the lungs in both experimental and control groups. MnNPs reformulated as a more concentrated suspension will be explored to minimize the acute response through minimization of the liquid volume required, although careful attention must be devoted to the consequent stability of MnNPs in a more concentrated solution.

Conclusions

These studies demonstrate the biocompatibility of MnNP both *in vitro* and *in vivo*, and provide evidence for enhanced TAM-targeting generated through the use of mannose as a targeting ligand on the particle surfaces. Here I provide evidence that these MnNP produce no significant toxicity when used *in vivo.* Incubating BMDMs with MnNP did not significantly decrease cell membrane viability and repeated, treatments in adult mice creates no acute kidney or liver damage. Furthermore, I showed that MnNP are effective at delivering fluorescently-labeled nucleotides to TAMs in spontaneously formed, primary mammary tumors. Additionally, mannose-targeting on the surface of the MnNP results in greater delivery of labeled nucleotides to ovarian tumor TAMs compared to non-targeted, hydroxyl-capped nanoparticles with the same core structure. Future studies will aim to further develop MnNP for biological applications and eventual clinical use, specifically utilizing MnNP to deliver active siRNAs to TAMs *in vivo* to knock down specific target proteins in key transcriptional pathways essential for creating the TAM phenotype and to activate an immunogenic, anti-tumor phenotype in this macrophage population.

CHAPTER 5

Summary and future work

The primary focus of my dissertation has been the development, optimization, and utilization of mannosylated, endosomal escape nanoparticles (MnNP) to modulate the phenotype of macrophages by delivering NF-κB specific siRNA. I hypothesized that by manipulating the NF-κB pathways in macrophages it is possible to create anti-tumor characteristics in these cells. I have shown that the MnNP effectively deliver functional siRNA to macrophages and that nucleotide delivery is enhanced by the targeting moiety, mannose, which targets the mannose receptor on the surface of tissue regenerative and tumor associated macrophages. I have also developed a novel method of activating phenotype controlling, transcriptional pathways in macrophages by knocking down an inhibitor of the pathway with siRNA. Preliminary evidence shows that activation of the classical NF-κB pathway in this manner results in a decrease in mRNA for tumor-supportive cytokines and an increase in an important activated T-cell recruiting cytokine. Finally, I have shown that these particles are biocompatible both *in vitro* and *in vivo*, and that the mannosylated particles facilitate enhanced delivery of nucleotide sequences to tumor associated macrophages in multiple *in vivo* murine models of human cancers.

Tumor associated macrophages (TAMs) have been implicated as one of the most prevalent and impactful types of immune cells in the tumor related stroma. TAMs produce an array of cytokines which provide support to nearby tumor cells, suppress classical immune activation in the tumor thereby helping tumor cells evade immune surveillance, and participate in tumor cell extravasation and metastasis. TAMs also display increased amounts of the mannose receptor. By functionalizing the surface of the nanoparticles with mannose, it is possible to enhance uptake of the siRNA loaded particles in TAMs and in *in vitro* cell models of TAMs.

In comparative transfection experiments with commercial agents, MnNP performed similarly to the commercial agents in transfection and knockdown efficacy, with the additional potential for *in vivo* use. While commercial agents deliver moderate amounts of nucleotide to a large population of cells, MnNP deliver greater amounts of nucleotide to a smaller subset of cells, consistent with enhanced delivery to the subset of cells expressing greater amounts of the target endosomal receptor. MnNP are also taken up faster and in greater amounts than untargeted, hydroxyl-capped nanoparticles (OHNP) with the same core structure.

I have used MnNP to deliver siRNA to macrophages *in vitro* in order to validate a novel strategy for abrogating the TAM phenotype and activating a classical immune response in macrophages. This strategy entails delivering siRNA for the inhibitor of the classical NF-κB pathway to macrophages and activating classical NF-κB signaling by knocking down the inhibitor at the mRNA level. qRT-PCR analysis indicates that this methodology has the potential to activate T-cell recruitment by these macrophages, decrease immunoinhibitory molecules and markers, and increase the macrophages' ability to respond to inflammatory signals. The intent of this therapeutic strategy would ultimately be to disrupt the TAM-generating, positive feedback loop between macrophages and tumor cells, and activate tumor immunity.

During the course of my investigation into the effects of NF-κB mediated manipulation of macrophage phenotype, I have collected data documenting the effects of knocking down specific NF-κB proteins by targeting the mRNA for these proteins for degradation by activating the RNAi pathway. I have also investigated the complex interplay between tumor cells and macrophages, with special focus on the contribution that NF-κB modulation makes to the TAM phenotype. Current research into the factors affecting TAM-tumor cell interaction tend to either use genomic or proteomic analysis to visualize the contribution of hundreds or thousands of factors, or investigates the effects of one or two cytokines in great detail. I believe that it is likely that the TAM phenotype is not generated by the activity of one or two cytokines acting on tumor-resident macrophages. Also, it is unlikely that every cytokine produced by TAMs and tumor cells has the same magnitude of effect on TAM-tumor interactions. One possible future direction

for this work is to analyze the different factors contributing to TAM-tumor cell interaction by performing meta-analysis of existing work and principle component analysis of the different cytokines known to both act on the NF-κB pathways and contribute to the TAM phenotype. MnNP would be a useful tool for investigating the effects of knocking down specific components of this system, and analyzing the effects of that knockdown. This analysis could result in a functional model of the role NF-κB plays in generating and sustaining the TAM phenotype.

I have also performed *in vivo* experiments demonstrating the enhanced uptake of MnNP by macrophages in several mouse models of human cancer. MnNP are highly biocompatible both *in vitro* and *in vivo*. Repeated intravenous doses of MnNP loaded with short nucleotide sequences do not cause acute liver or kidney damage in mice. In a spontaneous mouse model of breast cancer, intra-tumoral injections of MnNP loaded with fluorescently labeled nucleotides resulted in enhanced uptake of the nucleotides compared to phagocytic uptake of the same amount of free nucleotide. In a disseminated, late-stage ovarian tumor model, MnNP were taken up by macrophages in the solid tumor implants while there was no significant uptake of untargeted particles. This was likely due to non-specific uptake of the OHNP by the millions of phagocytic immune cells in the ovarian ascites fluid. Finally, MnNP were delivered via intratracheal intubation to mouse lungs in a tail vein injected, lung metastasis model of breast cancer. MnNP uptake was enhanced in macrophages compared to OHNP. Granulocytes and monocytes had no preference for a specific type of particle, indicating that while these cells internalized the particles through non-specific mechanisms, MnNP were taken up through a mannose dependent mechanism.

Currently, there is enough evidence to support the suppositions that MnNP-delivered siRNA can manipulate macrophage phenotype, and that MnNP are capable of enhanced delivery to TAMs *in vivo*. The next logical step for demonstrating the therapeutic potential of MnNP for macrophage phenotype editing is to deliver functional siRNA to TAMs *in vivo*. Dosing regimens can be informed by previous experiments and modification of TAM phenotype could be confirmed by isolating the TAMs from the primary tumors or metastases and analyzing macrophage phenotype with a flow cytometry panel and/or genomic analysis.

In order to show true therapeutic efficacy, Kaplan-Meier analysis of animal survival following siRNA delivery could also be performed.

Finally, mannose receptor expressing macrophages are not only implicated in pathological behavior in the context of solid tumors. MnNP could be used to target $CD206^{+}$ macrophages in other pathologies as well. For example, a population of M2-like macrophages has recently been implicated in the dysregulation of iron homeostasis in adipose tissue. Elucidating the effects of these $CD206^{+}$ cells could have implications for the treatment of obesity, type 2 diabetes, and other metabolic disorders. I am currently working in an advisory capacity with a research group led by Dr. Alyssa Hasty in the department of Molecular Physiology and Biophysics to facilitate the use of MnNP to investigate the contributions of these adipose macrophages to the dysregulation of iron homeostasis.

REFERENCES

1 B. Z. Qian, and J. W. Pollard, 'Macrophage Diversity Enhances Tumor Progression and Metastasis', *Cell,* 141 (2010), 39-51.

2 A. Mantovani, S. Sozzani, M. Locati, P. Allavena, and A. Sica, 'Macrophage Polarization: Tumor-Associated Macrophages as a Paradigm for Polarized M2 Mononuclear Phagocytes', *Trends Immunol,* 23 (2002), 549-55.

3 A. Oeckinghaus, M. S. Hayden, and S. Ghosh, 'Crosstalk in Nf-Kappab Signaling Pathways', *Nat Immunol,* 12 (2011), 695-708.

4 B. Qian, Y. Deng, J. H. Im, R. J. Muschel, Y. Zou, J. Li, R. A. Lang, and J. W. Pollard, 'A Distinct Macrophage Population Mediates Metastatic Breast Cancer Cell Extravasation, Establishment and Growth', *PLoS One,* 4 (2009), e6562.

5 J. W. Pollard, 'Tumour-Educated Macrophages Promote Tumour Progression and Metastasis', *Nat Rev Cancer,* 4 (2004), 71-8.

6 J. Condeelis, and J. W. Pollard, 'Macrophages: Obligate Partners for Tumor Cell Migration, Invasion, and Metastasis', *Cell,* 124 (2006), 263-6.

7 L. M. Coussens, and Z. Werb, 'Inflammation and Cancer', *Nature,* 420 (2002), 860-7.

8 Y. Ben-Neriah, and M. Karin, 'Inflammation Meets Cancer, with Nf-Kappab as the Matchmaker', *Nat Immunol,* 12 (2011), 715-23.

9 J. A. DiDonato, F. Mercurio, and M. Karin, 'Nf-Kappab and the Link between Inflammation and Cancer', *Immunol Rev,* 246 (2012), 379-400.

10 A. Fire, S. Xu, M. K. Montgomery, S. A. Kostas, S. E. Driver, and C. C. Mello, 'Potent and Specific Genetic Interference by Double-Stranded Rna in Caenorhabditis Elegans', *Nature,* 391 (1998), 806-11.

11 M. E. Davis, J. E. Zuckerman, C. H. Choi, D. Seligson, A. Tolcher, C. A. Alabi, Y. Yen, J. D. Heidel, and A. Ribas, 'Evidence of Rnai in Humans from Systemically Administered Sirna Via Targeted Nanoparticles', *Nature,* 464 (2010), 1067-70.

12 P. Allavena, M. Chieppa, G. Bianchi, G. Solinas, M. Fabbri, G. Laskarin, and A. Mantovani, 'Engagement of the Mannose Receptor by Tumoral Mucins Activates an Immune Suppressive Phenotype in Human Tumor-Associated Macrophages', *Clin Dev Immunol,* 2010 (2010), 547179.

13 S. S. Yu, C. M. Lau, W. J. Barham, H. M. Onishko, C. E. Nelson, H. Li, C. A. Smith, F. E. Yull, C. L. Duvall, and T. D. Giorgio, 'Macrophage-Specific Rna Interference Targeting Via "Click", Mannosylated Polymeric Micelles', *Mol Pharm,* 10 (2013), 975-87.

14 J. W. Pollard, 'Trophic Macrophages in Development and Disease', *Nat Rev Immunol,* 9 (2009), 259-70.

15 L. S. Ojalvo, W. King, D. Cox, and J. W. Pollard, 'High-Density Gene Expression Analysis of Tumor-Associated Macrophages from Mouse Mammary Tumors', *Am J Pathol,* 174 (2009), 1048-64.

16 T. Zabuawala, D. A. Taffany, S. M. Sharma, A. Merchant, B. Adair, R. Srinivasan, T. J. Rosol, S. Fernandez, K. Huang, G. Leone, and M. C. Ostrowski, 'An Ets2-Driven Transcriptional Program in Tumor-Associated Macrophages Promotes Tumor Metastasis', *Cancer Res,* 70 (2010), 1323-33.

17 A. Mantovani, and A. Sica, 'Macrophages, Innate Immunity and Cancer: Balance, Tolerance, and Diversity', *Curr Opin Immunol,* 22 (2010), 231-7.

18 E. Y. Lin, A. V. Nguyen, R. G. Russell, and J. W. Pollard, 'Colony-Stimulating Factor 1 Promotes Progression of Mammary Tumors to Malignancy', *J Exp Med,* 193 (2001), 727-40.

19 S. Gordon, 'Alternative Activation of Macrophages', *Nat Rev Immunol,* 3 (2003), 23-35.
20 F. R. Greten, L. Eckmann, T. F. Greten, J. M. Park, Z. W. Li, L. J. Egan, M. F. Kagnoff, and M. Karin, 'Ikkbeta Links Inflammation and Tumorigenesis in a Mouse Model of Colitis-Associated Cancer', *Cell,* 118 (2004), 285-96.
21 J. D. Hudson, M. A. Shoaibi, R. Maestro, A. Carnero, G. J. Hannon, and D. H. Beach, 'A Proinflammatory Cytokine Inhibits P53 Tumor Suppressor Activity', *J Exp Med,* 190 (1999), 1375-82.
22 M. Karin, and F. R. Greten, 'Nf-Kappab: Linking Inflammation and Immunity to Cancer Development and Progression', *Nat Rev Immunol,* 5 (2005), 749-59.
23 S. C. Sun, 'The Noncanonical Nf-Kappab Pathway', *Immunol Rev,* 246 (2012), 125-40.
24 F. Weih, and J. Caamano, 'Regulation of Secondary Lymphoid Organ Development by the Nuclear Factor-Kappab Signal Transduction Pathway', *Immunol Rev,* 195 (2003), 91-105.
25 G. Xiao, A. Fong, and S. C. Sun, 'Induction of P100 Processing by Nf-Kappab-Inducing Kinase Involves Docking Ikappab Kinase Alpha (Ikkalpha) to P100 and Ikkalpha-Mediated Phosphorylation', *J Biol Chem,* 279 (2004), 30099-105.
26 G. Liao, M. Zhang, E. W. Harhaj, and S. C. Sun, 'Regulation of the Nf-Kappab-Inducing Kinase by Tumor Necrosis Factor Receptor-Associated Factor 3-Induced Degradation', *J Biol Chem,* 279 (2004), 26243-50.
27 S. Beinke, and S. C. Ley, 'Functions of Nf-Kappab1 and Nf-Kappab2 in Immune Cell Biology', *Biochem J,* 382 (2004), 393-409.
28 F. Chellat, Y. Merhi, A. Moreau, and L. Yahia, 'Therapeutic Potential of Nanoparticulate Systems for Macrophage Targeting', *Biomaterials,* 26 (2005), 7260-75.
29 Y. Luo, H. Zhou, J. Krueger, C. Kaplan, S. H. Lee, C. Dolman, D. Markowitz, W. Wu, C. Liu, R. A. Reisfeld, and R. Xiang, 'Targeting Tumor-Associated Macrophages as a Novel Strategy against Breast Cancer', *J Clin Invest,* 116 (2006), 2132-41.
30 C. Boyer, V. Bulmus, T. P. Davis, V. Ladmiral, J. Liu, and S. Perrier, 'Bioapplications of Raft Polymerization', *Chem Rev,* 109 (2009), 5402-36.
31 A. J. Convertine, D. S. Benoit, C. L. Duvall, A. S. Hoffman, and P. S. Stayton, 'Development of a Novel Endosomolytic Diblock Copolymer for Sirna Delivery', *J Control Release,* 133 (2009), 221-9.
32 H. C. Kolb, and K. B. Sharpless, 'The Growing Impact of Click Chemistry on Drug Discovery', *Drug Discov Today,* 8 (2003), 1128-37.
33 S. M. Elbashir, J. Harborth, W. Lendeckel, A. Yalcin, K. Weber, and T. Tuschl, 'Duplexes of 21-Nucleotide Rnas Mediate Rna Interference in Cultured Mammalian Cells', *Nature,* 411 (2001), 494-8.
34 M. E. Davis, 'The First Targeted Delivery of Sirna in Humans Via a Self-Assembling, Cyclodextrin Polymer-Based Nanoparticle: From Concept to Clinic', *Mol Pharm,* 6 (2009), 659-68.
35 A. D. Judge, M. Robbins, I. Tavakoli, J. Levi, L. Hu, A. Fronda, E. Ambegia, K. McClintock, and I. MacLachlan, 'Confirming the Rnai-Mediated Mechanism of Action of Sirna-Based Cancer Therapeutics in Mice', *J Clin Invest,* 119 (2009), 661-73.
36 J. P. Behr, 'The Proton Sponge: A Trick to Enter Cells That Viruses Did Not Exploit', *Chimia,* 51 (1997), 34-36.
37 A. J. Convertine, C. Diab, M. Prieve, A. Paschal, A. S. Hoffman, P. H. Johnson, and P. S. Stayton, 'Ph-Responsive Polymeric Micelle Carriers for Sirna Drugs', *Biomacromolecules,* 11 (2010), 2904-11.
38 B. C. Evans, C. E. Nelson, S. S. Yu, K. R. Beavers, A. J. Kim, H. Li, H. M. Nelson, T. D. Giorgio, and C. L. Duvall, 'Ex Vivo Red Blood Cell Hemolysis Assay for the Evaluation of Ph-Responsive Endosomolytic Agents for Cytosolic Delivery of Biomacromolecular Drugs', *J Vis Exp* (2013), e50166.

39 H. Li, S. S. Yu, M. Miteva, C. E. Nelson, T. Werfel, T. D. Giorgio, and C. L. Duvall, 'Matrix Metalloproteinase Responsive, Proximity-Activated Polymeric Nanoparticles for Sirna Delivery', *Advanced Functional Materials,* 23 (2013), 3040-52.

40 P. D. Stahl, and R. A. Ezekowitz, 'The Mannose Receptor Is a Pattern Recognition Receptor Involved in Host Defense', *Curr Opin Immunol,* 10 (1998), 50-5.

41 B. L. Largent, K. M. Walton, C. A. Hoppe, Y. C. Lee, and R. L. Schnaar, 'Carbohydrate-Specific Adhesion of Alveolar Macrophages to Mannose-Derivatized Surfaces', *J Biol Chem,* 259 (1984), 1764-9.

42 L. Connelly, A. T. Jacobs, M. Palacios-Callender, S. Moncada, and A. J. Hobbs, 'Macrophage Endothelial Nitric-Oxide Synthase Autoregulates Cellular Activation and Pro-Inflammatory Protein Expression', *J Biol Chem,* 278 (2003), 26480-7.

43 L. Connelly, W. Barham, H. M. Onishko, L. Chen, T. P. Sherrill, T. Zabuawala, M. C. Ostrowski, T. S. Blackwell, and F. E. Yull, 'Nf-Kappab Activation within Macrophages Leads to an Anti-Tumor Phenotype in a Mammary Tumor Lung Metastasis Model', *Breast Cancer Res,* 13 (2011), R83.

44 L. Connelly, W. Barham, H. M. Onishko, T. Sherrill, L. A. Chodosh, T. S. Blackwell, and F. E. Yull, 'Inhibition of Nf-Kappa B Activity in Mammary Epithelium Increases Tumor Latency and Decreases Tumor Burden', *Oncogene,* 30 (2011), 1402-12.

45 M. Y. Fong, and S. S. Kakar, 'Ovarian Cancer Mouse Models: A Summary of Current Models and Their Limitations', *J Ovarian Res,* 2 (2009), 12.

46 F. Porcheray, S. Viaud, A. C. Rimaniol, C. Leone, B. Samah, N. Dereuddre-Bosquet, D. Dormont, and G. Gras, 'Macrophage Activation Switching: An Asset for the Resolution of Inflammation', *Clin Exp Immunol,* 142 (2005), 481-9.

47 P. R. Crocker, and S. Gordon, 'Isolation and Characterization of Resident Stromal Macrophages and Hematopoietic Cell Clusters from Mouse Bone Marrow', *J Exp Med,* 162 (1985), 993-1014.

48 L. A. Dethloff, and B. E. Lehnert, 'Pulmonary Interstitial Macrophages: Isolation and Flow Cytometric Comparisons with Alveolar Macrophages and Blood Monocytes', *J Leukoc Biol,* 43 (1988), 80-90.

49 M. E. Key, J. E. Talmadge, W. E. Fogler, C. Bucana, and I. J. Fidler, 'Isolation of Tumoricidal Macrophages from Lung Melanoma Metastases of Mice Treated Systemically with Liposomes Containing a Lipophilic Derivative of Muramyl Dipeptide', *J Natl Cancer Inst,* 69 (1982), 1198-98.

50 M. A. Schon-Hegrad, and P. G. Holt, 'Improved Method for the Isolation of Purified Mouse Peritoneal Macrophages', *J Immunol Methods,* 43 (1981), 169-73.

51 J. B. Yee, and J. C. Hutson, 'Testicular Macrophages: Isolation, Characterization and Hormonal Responsiveness', *Biol Reprod,* 29 (1983), 1319-26.

52 E. Y. Lin, J. G. Jones, P. Li, L. Zhu, K. D. Whitney, W. J. Muller, and J. W. Pollard, 'Progression to Malignancy in the Polyoma Middle T Oncoprotein Mouse Breast Cancer Model Provides a Reliable Model for Human Diseases', *Am J Pathol,* 163 (2003), 2113-26.

53 S. Cao, X. Zhang, J. P. Edwards, and D. M. Mosser, 'Nf-Kappab1 (P50) Homodimers Differentially Regulate Pro- and Anti-Inflammatory Cytokines in Macrophages', *J Biol Chem,* 281 (2006), 26041-50.

54 M. A. Cheever, 'Twelve Immunotherapy Drugs That Could Cure Cancers', *Immunol Rev,* 222 (2008), 357-68.

55 M. Kalos, and C. H. June, 'Adoptive T Cell Transfer for Cancer Immunotherapy in the Era of Synthetic Biology', *Immunity,* 39 (2013), 49-60.

56 D. G. DeNardo, D. J. Brennan, E. Rexhepaj, B. Ruffell, S. L. Shiao, S. F. Madden, W. M. Gallagher, N. Wadhwani, S. D. Keil, S. A. Junaid, H. S. Rugo, E. S. Hwang, K. Jirstrom, B. L. West, and L. M. Coussens, 'Leukocyte Complexity Predicts Breast Cancer Survival and Functionally Regulates Response to Chemotherapy', *Cancer Discov,* 1 (2011), 54-67.

57 M. Baj-Krzyworzeka, J. Baran, R. Szatanek, D. Stankiewicz, M. Siedlar, and M. Zembala, 'Prevention and Reversal of Tumor Cell-Induced Monocyte Deactivation by Cytokines, Purified Protein Derivative (Ppd), and Anti-Il-10 Antibody', *Cancer Immun,* 4 (2004), 8.

58 A. Sica, A. Saccani, B. Bottazzi, N. Polentarutti, A. Vecchi, J. van Damme, and A. Mantovani, 'Autocrine Production of Il-10 Mediates Defective Il-12 Production and Nf-Kappa B Activation in Tumor-Associated Macrophages', *J Immunol,* 164 (2000), 762-7.

59 J. A. Van Ginderachter, K. Movahedi, G. Hassanzadeh Ghassabeh, S. Meerschaut, A. Beschin, G. Raes, and P. De Baetselier, 'Classical and Alternative Activation of Mononuclear Phagocytes: Picking the Best of Both Worlds for Tumor Promotion', *Immunobiology,* 211 (2006), 487-501.

60 D. G. DeNardo, J. B. Barreto, P. Andreu, L. Vasquez, D. Tawfik, N. Kolhatkar, and L. M. Coussens, 'Cd4(+) T Cells Regulate Pulmonary Metastasis of Mammary Carcinomas by Enhancing Protumor Properties of Macrophages', *Cancer Cell,* 16 (2009), 91-102.

61 E. Y. Lin, and J. W. Pollard, 'Tumor-Associated Macrophages Press the Angiogenic Switch in Breast Cancer', *Cancer Res,* 67 (2007), 5064-6.

62 C. Nathan, L. Brukner, G. Kaplan, J. Unkeless, and Z. Cohn, 'Role of Activated Macrophages in Antibody-Dependent Lysis of Tumor Cells', *J Exp Med,* 152 (1980), 183-97.

63 C. Nathan, and Z. Cohn, 'Role of Oxygen-Dependent Mechanisms in Antibody-Induced Lysis of Tumor Cells by Activated Macrophages', *J Exp Med,* 152 (1980), 198-208.

64 R. E. Bellas, M. J. FitzGerald, N. Fausto, and G. E. Sonenshein, 'Inhibition of Nf-Kappa B Activity Induces Apoptosis in Murine Hepatocytes', *Am J Pathol,* 151 (1997), 891-6.

65 G. Bonizzi, and M. Karin, 'The Two Nf-Kappab Activation Pathways and Their Role in Innate and Adaptive Immunity', *Trends Immunol,* 25 (2004), 280-8.

66 S. S. Makarov, 'Nf-Kappab as a Therapeutic Target in Chronic Inflammation: Recent Advances', *Mol Med Today,* 6 (2000), 441-8.

67 N. Fujiwara, and K. Kobayashi, 'Macrophages in Inflammation', *Curr Drug Targets Inflamm Allergy,* 4 (2005), 281-6.

68 B. Levkau, M. Scatena, C. M. Giachelli, R. Ross, and E. W. Raines, 'Apoptosis Overrides Survival Signals through a Caspase-Mediated Dominant-Negative Nf-Kappa B Loop', *Nat Cell Biol,* 1 (1999), 227-33.

69 L. J. Pagliari, H. Perlman, H. Liu, and R. M. Pope, 'Macrophages Require Constitutive Nf-Kappab Activation to Maintain A1 Expression and Mitochondrial Homeostasis', *Mol Cell Biol,* 20 (2000), 8855-65.

70 R. Koike, T. Nishimura, R. Yasumizu, H. Tanaka, Y. Hataba, Y. Hataba, T. Watanabe, S. Miyawaki, and M. Miyasaka, 'The Splenic Marginal Zone Is Absent in Alymphoplastic Aly Mutant Mice', *Eur J Immunol,* 26 (1996), 669-75.

71 S. Miyawaki, Y. Nakamura, H. Suzuka, M. Koba, R. Yasumizu, S. Ikehara, and Y. Shibata, 'A New Mutation, Aly, That Induces a Generalized Lack of Lymph Nodes Accompanied by Immunodeficiency in Mice', *Eur J Immunol,* 24 (1994), 429-34.

72 Y. Wang, X. Mo, M. G. Piper, H. Wang, N. L. Parinandi, D. Guttridge, and C. B. Marsh, 'M-Csf Induces Monocyte Survival by Activating Nf-Kappab P65 Phosphorylation at Ser276 Via Protein Kinase C', *PLoS One,* 6 (2011), e28081.

73 J. W. Fuseler, D. M. Merrill, J. A. Rogers, M. B. Grisham, and R. E. Wolf, 'Analysis and Quantitation of Nf-Kappa B Nuclear Translocation in Tumor Necrosis Factor Alpha (Tnf-Alpha) Activated Vascular Endothelial Cells', *Microscopy and Microanalysis,* 12 (2006), 269-76.

74 C. Roos, A. Wicovsky, N. Muller, S. Salzmann, T. Rosenthal, H. Kalthoff, A. Trauzold, A. Seher, F. Henkler, C. Kneitz, and H. Wajant, 'Soluble and Transmembrane Tnf-Like Weak Inducer of Apoptosis Differentially Activate the Classical and Noncanonical Nf-Kappa B Pathway', *J Immunol,* 185 (2010), 1593-605.

75 U. Chattopadhyay, S. Bhattacharyya, and N. G. Chakrabarty, 'Tumor Associated Macrophage Mediated Lysis of Autologous Tumor Cells', *Neoplasma,* 33 (1986), 157-65.
76 G. W. Cox, 'Assay for Macrophage-Mediated Anti-Tumor Cytotoxicity', *Curr Protoc Immunol,* Chapter 14 (2001), Unit 14 7.
77 M. Muller, S. Carter, M. J. Hofer, and I. L. Campbell, 'Review: The Chemokine Receptor Cxcr3 and Its Ligands Cxcl9, Cxcl10 and Cxcl11 in Neuroimmunity--a Tale of Conflict and Conundrum', *Neuropathol Appl Neurobiol,* 36 (2010), 368-87.
78 K. Palmer, M. Hitt, P. C. Emtage, S. Gyorffy, and J. Gauldie, 'Combined Cxc Chemokine and Interleukin-12 Gene Transfer Enhances Antitumor Immunity', *Gene Ther,* 8 (2001), 282-90.
79 C. S. Tannenbaum, R. Tubbs, D. Armstrong, J. H. Finke, R. M. Bukowski, and T. A. Hamilton, 'The Cxc Chemokines Ip-10 and Mig Are Necessary for Il-12-Mediated Regression of the Mouse Renca Tumor', *J Immunol,* 161 (1998), 927-32.
80 M. E. Dudley, and S. A. Rosenberg, 'Adoptive-Cell-Transfer Therapy for the Treatment of Patients with Cancer', *Nat Rev Cancer,* 3 (2003), 666-75.
81 A. Mantovani, A. Sica, S. Sozzani, P. Allavena, A. Vecchi, and M. Locati, 'The Chemokine System in Diverse Forms of Macrophage Activation and Polarization', *Trends Immunol,* 25 (2004), 677-86.
82 L. Armstrong, N. Jordan, and A. Millar, 'Interleukin 10 (Il-10) Regulation of Tumour Necrosis Factor Alpha (Tnf-Alpha) from Human Alveolar Macrophages and Peripheral Blood Monocytes', *Thorax,* 51 (1996), 143-9.
83 F. Driessler, K. Venstrom, R. Sabat, K. Asadullah, and A. J. Schottelius, 'Molecular Mechanisms of Interleukin-10-Mediated Inhibition of Nf-Kappab Activity: A Role for P50', *Clin Exp Immunol,* 135 (2004), 64-73.
84 S. T. Smale, 'Hierarchies of Nf-Kappab Target-Gene Regulation', *Nat Immunol,* 12 (2011), 689-94.
85 M. Saraiva, and A. O'Garra, 'The Regulation of Il-10 Production by Immune Cells', *Nat Rev Immunol,* 10 (2010), 170-81.
86 M. L. Fiani, J. Beitz, D. Turvy, J. S. Blum, and P. D. Stahl, 'Regulation of Mannose Receptor Synthesis and Turnover in Mouse J774 Macrophages', *J Leukoc Biol,* 64 (1998), 85-91.
87 R. A. Ezekowitz, K. Sastry, P. Bailly, and A. Warner, 'Molecular Characterization of the Human Macrophage Mannose Receptor: Demonstration of Multiple Carbohydrate Recognition-Like Domains and Phagocytosis of Yeasts in Cos-1 Cells', *J Exp Med,* 172 (1990), 1785-94.
88 Y. Mao, E. T. Keller, D. H. Garfield, K. Shen, and J. Wang, 'Stromal Cells in Tumor Microenvironment and Breast Cancer', *Cancer Metastasis Rev,* 32 (2013), 303-15.
89 M. Heusinkveld, and S. H. van der Burg, 'Identification and Manipulation of Tumor Associated Macrophages in Human Cancers', *J Transl Med,* 9 (2011), 216.
90 W. Han, M. Joo, M. B. Everhart, J. W. Christman, F. E. Yull, and T. S. Blackwell, 'Myeloid Cells Control Termination of Lung Inflammation through the Nf-Kappab Pathway', *Am J Physiol Lung Cell Mol Physiol,* 296 (2009), L320-7.
91 R. Zaynagetdinov, T. P. Sherrill, V. V. Polosukhin, W. Han, J. A. Ausborn, A. G. McLoed, F. B. McMahon, L. A. Gleaves, A. L. Degryse, G. T. Stathopoulos, F. E. Yull, and T. S. Blackwell, 'A Critical Role for Macrophages in Promotion of Urethane-Induced Lung Carcinogenesis', *J Immunol,* 187 (2011), 5703-11.
92 H. Maeda, 'The Enhanced Permeability and Retention (Epr) Effect in Tumor Vasculature: The Key Role of Tumor-Selective Macromolecular Drug Targeting', *Adv Enzyme Regul,* 41 (2001), 189-207.
93 W. Wijagkanalan, S. Kawakami, M. Takenaga, R. Igarashi, F. Yamashita, and M. Hashida, 'Efficient Targeting to Alveolar Macrophages by Intratracheal Administration of Mannosylated Liposomes in Rats', *J Control Release,* 125 (2008), 121-30.

94 R. Zaynagetdinov, T. P. Sherrill, P. L. Kendall, B. H. Segal, K. P. Weller, R. M. Tighe, and T. S. Blackwell, 'Identification of Myeloid Cell Subsets in Murine Lungs Using Flow Cytometry', *Am J Respir Cell Mol Biol,* 49 (2013), 180-9.

95 D. Pilling, T. Fan, D. Huang, B. Kaul, and R. H. Gomer, 'Identification of Markers That Distinguish Monocyte-Derived Fibrocytes from Monocytes, Macrophages, and Fibroblasts', *PLoS One,* 4 (2009), e7475.

96 W. Xu, N. Schlagwein, A. Roos, T. K. van den Berg, M. R. Daha, and C. van Kooten, 'Human Peritoneal Macrophages Show Functional Characteristics of M-Csf-Driven Anti-Inflammatory Type 2 Macrophages', *Eur J Immunol,* 37 (2007), 1594-9.

97 P. Szlosarek, K. A. Charles, and F. R. Balkwill, 'Tumour Necrosis Factor-Alpha as a Tumour Promoter', *Eur J Cancer,* 42 (2006), 745-50.

98 P. W. Szlosarek, and F. R. Balkwill, 'Tumour Necrosis Factor Alpha: A Potential Target for the Therapy of Solid Tumours', *Lancet Oncol,* 4 (2003), 565-73.

99 W. Strober, 'Trypan Blue Exclusion Test of Cell Viability', *Curr Protoc Immunol,* Appendix 3 (2001), Appendix 3B.

100 R. Mauisse, D. De Semir, H. Emamekhoo, B. Bedayat, A. Abdolmohammadi, H. Parsi, and D. C. Gruenert, 'Comparative Transfection of DNA into Primary and Transformed Mammalian Cells from Different Lineages', *BMC Biotechnology,* 10 (2010).

101 F. C. Brosius, 3rd, C. E. Alpers, E. P. Bottinger, M. D. Breyer, T. M. Coffman, S. B. Gurley, R. C. Harris, M. Kakoki, M. Kretzler, E. H. Leiter, M. Levi, R. A. McIndoe, K. Sharma, O. Smithies, K. Susztak, N. Takahashi, T. Takahashi, and Consortium Animal Models of Diabetic Complications, 'Mouse Models of Diabetic Nephropathy', *J Am Soc Nephrol,* 20 (2009), 2503-12.

102 R. D. Leek, R. J. Landers, A. L. Harris, and C. E. Lewis, 'Necrosis Correlates with High Vascular Density and Focal Macrophage Infiltration in Invasive Carcinoma of the Breast', *Br J Cancer,* 79 (1999), 991-5.

103 K. Greish, 'Enhanced Permeability and Retention of Macromolecular Drugs in Solid Tumors: A Royal Gate for Targeted Anticancer Nanomedicines', *J Drug Target,* 15 (2007), 457-64.

104 J. Greenaway, R. Moorehead, P. Shaw, and J. Petrik, 'Epithelial-Stromal Interaction Increases Cell Proliferation, Survival and Tumorigenicity in a Mouse Model of Human Epithelial Ovarian Cancer', *Gynecol Oncol,* 108 (2008), 385-94.

105 T. Hagemann, J. Wilson, F. Burke, H. Kulbe, N. F. Li, A. Pluddemann, K. Charles, S. Gordon, and F. R. Balkwill, 'Ovarian Cancer Cells Polarize Macrophages toward a Tumor-Associated Phenotype', *J Immunol,* 176 (2006), 5023-32.

106 E. Schutyser, S. Struyf, P. Proost, G. Opdenakker, G. Laureys, B. Verhasselt, L. Peperstraete, I. Van de Putte, A. Saccani, P. Allavena, A. Mantovani, and J. Van Damme, 'Identification of Biologically Active Chemokine Isoforms from Ascitic Fluid and Elevated Levels of Ccl18/Pulmonary and Activation-Regulated Chemokine in Ovarian Carcinoma', *J Biol Chem,* 277 (2002), 24584-93.

107 A. Sica, A. Saccani, B. Bottazzi, S. Bernasconi, P. Allavena, B. Gaetano, F. Fei, G. LaRosa, C. Scotton, F. Balkwill, and A. Mantovani, 'Defective Expression of the Monocyte Chemotactic Protein-1 Receptor Ccr2 in Macrophages Associated with Human Ovarian Carcinoma', *J Immunol,* 164 (2000), 733-8.

108 M. J. Turk, D. J. Waters, and P. S. Low, 'Folate-Conjugated Liposomes Preferentially Target Macrophages Associated with Ovarian Carcinoma', *Cancer Lett,* 213 (2004), 165-72.

109 A. J. Wilson, W. Barham, J. Saskowski, O. Tikhomirov, L. Chen, H. J. Lee, F. Yull, and D. Khabele, 'Tracking Nf-Kappab Activity in Tumor Cells During Ovarian Cancer Progression in a Syngeneic Mouse Model', *J Ovarian Res,* 6 (2013), 63.

110 O. B. Garbuzenko, M. Saad, S. Betigeri, M. Zhang, A. A. Vetcher, V. A. Soldatenkov, D. C. Reimer, V. P. Pozharov, and T. Minko, 'Intratracheal Versus Intravenous Liposomal Delivery of Sirna, Antisense Oligonucleotides and Anticancer Drug', *Pharm Res,* 26 (2009), 382-94.